

Article

Analyzing Geospatial Cost Variability of Hybrid Solar–Gravity Storage System in High-Curtailment Suburban Areas

Soumya Basu , Tetsuhito Hoshino and Hideyuki Okumura * 

Graduate School of Energy Science, Kyoto University, Yoshida Honmachi, Sakyo-ku, Kyoto 6068501, Japan; soumya.basu.28e@st.kyoto-u.ac.jp (S.B.); hoshino@social-system.energy.kyoto-u.ac.jp (T.H.)

* Correspondence: okumura@energy.kyoto-u.ac.jp

Abstract: The increased decentralization of renewable energy has increased curtailment rates in stagnating demand zones, increasing the levelized cost of energy (LCOE). The geographically dynamic nature of gravity energy storage (GES) is emerging in the field of mechanical energy storage, over pumped hydro. However, GES costs vary geospatially, specifically in decentralized suburban areas, due to the impact of urban socioeconomics. This study aims to find a mathematical approximation of a cost-optimized location for suburban Solar–GES hybrid systems in curtailment-prone areas. A multi-parameterization model mathematically programmed land, transmission, supply chain and excavation costs into geospatial matrix approximations for suburban areas of 2500 km² in Fukuoka and Ibaraki in Japan. It was found that SPV-GES location-dependent costs were mainly affected by distance from the city's economic center and flat plains in suburbs, and supply chain and transmission costs optimized the location-dependent cost for GES at a specific point. It was also found that flat terrains were more economical than mountainous terrains due to high GES supply chain costs. With GES found to be cost-competitive compared to other storage technologies in Japan, this study reveals that GES introduction benefits the LCOE of suburban, decentralized SPV when curtailment is >50% irrespective of terrain.

Keywords: solar photovoltaic; decentralized; gravity storage; location-dependent costs; suburban; cost optimization; curtailment mitigation; levelized cost of energy



Citation: Basu, S.; Hoshino, T.; Okumura, H. Analyzing Geospatial Cost Variability of Hybrid Solar–Gravity Storage System in High-Curtailment Suburban Areas. *Energies* **2024**, *17*, 2162. <https://doi.org/10.3390/en17092162>

Academic Editors: Wen-Hsien Tsai and Chu-Lun Hsieh

Received: 31 March 2024

Revised: 26 April 2024

Accepted: 29 April 2024

Published: 30 April 2024



Copyright: © 2024 by the authors. Licensee MDPI, Basel, Switzerland. This article is an open access article distributed under the terms and conditions of the Creative Commons Attribution (CC BY) license (<https://creativecommons.org/licenses/by/4.0/>).

1. Introduction

In the struggle to achieve net zero emission targets, variable renewable energy sources (VREs) like wind and solar photovoltaic (SPV) have become the major options. Due to advanced methods of fabrication, semiconductor material synthesis and power loss reduction, the efficiency of SPV is increasing every day [1,2]. This has brought the levelized cost of energy (LCOE) of SPV lower than fossil fuels in several countries like China [3,4], Japan [5,6] and India [3,7]. Socioeconomic analysis has also been carried out to reduce the LCOE of SPV further in terms of social acceptance [6], internal rate of returns (IRR) [8,9] and spatial cost variability [10]. However, in recent years, the rate of adoption of SPV power has increased manifold owing to the Paris Agreement's determined contributions and net zero targets [1,6], which has led to supply being significantly larger than demand, even during the non-peak production hours [11]. The capacity factors for SPV are 10–12% in countries with stagnating electricity demand like Japan and Germany [11–13]. Additionally, intermittency due to cloud covers and weather has also contributed to the curtailment of SPV production in high-PV-penetration areas with lower demand [14], while several policy simulations like time-of-day charging for electric vehicles [15] and subsidized time-of-day consumption (when SPV power is generated) [16], etc., have not been significant in increasing the capacity factors in curtailment-prone areas. This has the potential to increase the LCOE as more utility-scale SPV is introduced in line with net-zero commitments.

Energy storage technologies such as batteries and pumped hydro energy storage (PHES) have been considered for solving the diurnal intermittency of SPV and wind generation [17,18]. However, curtailment introduces a new challenge, which is far too expensive for existing battery technology. The challenge with PHES is that it has low geographical applicability and is constrained by location and capacity design [18]. Other types of mechanical storage such as flywheel energy storage (FES) [17] and compressed air energy storage (CAES) [19] are still under development. CAES is specifically very geographically constraining due to the requirement of natural salt caverns for large-scale curtailment storage. While VRE shows growth in the future, PHES and CAES will become increasingly limited in their applications, specifically in high-curtailment zones [20]. A major issue in storing curtailed VRE power is that the storage technology should be inexpensive, geographically dynamic and have a fast load response time and discharging time.

To address this issue, this study considers a recently researched mechanical storage system, gravity energy storage (GES), which stores electrical energy by converting it into the potential energy of a lifted weight, and generates electrical energy from potential energy by dropping the weight [21,22]. GES is an attractive technology, which many previous studies claim to be an alternative to PHES [23–25], specifically due to it being geographically dynamic. It can be constructed in abandoned mines, flat plains in suburban areas with minimal land requirements and mountainous areas by excavation [20,26,27]. However, to deploy GES in curtailment-prone zones, not only material optimization, but also economic optimization is imperative. The main problems that this study addresses are how the various socioeconomics of a city can affect GES costs geospatially, and whether the costs of SPV-GES systems can be optimized at a specific location.

The contributions of this study towards energy storage and SPV curtailment are divided into three aspects. The first aspect deals with the geographical viability of GES from the standpoint of location-dependent costs. Various cost analyses of GES systems have been performed in the existing literature, with material cost optimization being the primary focus [24,28]. The authors of [21] showed that steel and concrete are the most appropriate materials in terms of material density and procurement cost. This study employed reinforced concrete for the container and return pipe, and steel for the piston. A wind–GES life-cycle cost analysis was performed by a specific study, which revealed optimistic results [29]. The authors of [20] proposed a financial model for deploying utility-scale GES plants, which can be suited for high-curtailment zones. However, GES is hypothesized to be an improvement over PHES due to its non-limiting geographical applicability. Several costs like land, supply chain, transmission and labor are spatially variable even in a limited geographical distribution [10]. Moreover, construction and excavation are associated with the policies of local governing bodies, which determine costs according to geography and demography [30]. It is important to analyze the interplay of these costs according to location for GES installations, for both economic viability and efficient urban planning. This study fills the gap in the GES literature by mathematically approximating the location-dependent costs and providing an optimization algorithm.

The second aspect of this study is to provide a mathematical framework for analyzing the location dependency of LCOE for a hybrid GES-SPV system. With regard to the spatially variable installation costs of power plants, previous studies have focused on technical and social factors. For example, models have been presented to identify efficient supply points and optimize grid costs according to the location of supply points in decentralized networks [31]. The authors of [32] discuss technological advances aimed at reducing working hours, focusing on the location dependency of labor costs for VRE technologies. This research extends the multi-factor spatial parameterization (MUFSP) model presented by [10] for geolocating the optimal location of a utility-scale, suburban SPV plant. The MUFSP created by the authors of [10] is a cost simulation model that analyzes socioeconomic and geographic factors depending on the location of the SPV plant, which shows that location-dependent costs are mainly driven by the distance from the city's economic

center point. This study innovates the MUFSP model by modifying it for hybrid SPV-GES systems and introducing novel factors like excavation costs for mountainous terrains.

The central hypothesis is that every energy storage technology, including GES, will have variable location-dependent costs in any location. As decentralization progresses, VREs are going to be the only form of decentralized sources for net zero targets [33]. Decentralization will eventually require proximity to cities where substations are located, and so GES development aimed at curbing SPV (and VRE) curtailment will also have to be located in suburban areas. We further hypothesize that suburban GES installation cost variation will be significant with small changes in location, relative to a city's economic center, and an optimized cost location will be detectable. This can be supported by hedonic models, developed in past studies [10,34,35] for estimating land costs relative to a city's Central Business District (CBD). Our main contribution to the existing literature is to innovate urban socioeconomics into decentralized energy system economics. This study is the first to analyze the location dependency of the installation costs of an SPV-GES hybrid system in suburban areas. The mathematical model can reveal a theoretical basis that can be applicable to any hybrid system irrespective of location.

The third aspect of the research importantly considers developed economies where curtailment is caused by decreasing demands. Social factors affecting the location-dependent costs of SPV are completely different in developed countries with higher land and labor costs compared to developing countries [10,32,36,37]. Japan presents a peculiar net zero target, with a declining population and energy conservation policies of reducing demand by 18–20% by 2050 compared to 2015 energy consumption [38]. With curtailment already above 10% in the Japanese Kyushu grid [12], the LCOE of SPV will further increase without appropriate storage infrastructure. This study focuses on Fukuoka City, the largest population center in the Kyushu region of Japan [14], and Ibaraki City, in the vicinity of the Tokyo metropolitan area, the most populated city in the world [38]. Both these cities have stringent targets for decentralized power generation [39], making them the ideal location for testing the variability of the SPV-GES system's installation costs in suburban areas. Furthermore, the suburban geography of Fukuoka is mountainous, which is radically different from the flat suburban area of Ibaraki. Adopting the MUFSP approximation for mountainous terrain is a key novelty of this study. Another novelty is that multiple CBDs are considered in this study, which adds to hedonic modelling, with two in Fukuoka and five in Ibaraki [40]. This complex difference is critical to understand how the location-dependent costs of GES can vary in different suburban geographies and demographics. Figure 1 shows the locations of Fukuoka and Ibaraki on the map of Japan.

Thus, the main objective of this paper is to test the optimization of the location-dependent installation costs of hybrid SPV-GES systems in suburban areas of high-curtailment regions in a developed nation. We show how variations in costs can be different in separate suburban geographies and thereby provide a feasibility analysis of hybrid systems in curtailment-prone areas. While the existing literature has mainly focused on the LCOE [20,22,33], we also highlight the leveled cost of storage (LCOS) of hybrid SPV-GES systems and its spatial variations in suburban areas. We also consider LCOS variations of GES with the key financial factors of discount rates and lifetime generation coupled to demand and geospatial variability. Table 1 lists all the abbreviations and variable notations of this study.

Table 1. List of abbreviations and notations used in this study.

Abbreviation	Full Form/Meaning
VRE	Variable Renewable Energy
SPV	Solar Photovoltaic
GES	Gravity Energy Storage
P-GES	Piston (-type) Gravity Energy Storage

Table 1. Cont.

Abbreviation	Full Form/Meaning
LCOE	Levelized Cost of Energy
LCOS	Levelized Cost of Storage
IRR	Internal Rate of Return
PHES	Pumped Hydro Energy Storage
CAES	Compressed Air Energy Storage
FES	Flywheel Energy Storage
MUFSP	MUlti-Factor Spatial Parameterization
CBD	Central Business District
LDC	Load Distribution Center
Manu	Manufacturing Plant
SS	Substation
FP	Flat Point
MP	Mountain Point
GIS	Geographic Information System
NMC	Nickel–Manganese–Cobalt
LFP	Lithium–Ferrous–Phosphate
SDG	Sustainable Development Goals
ACSR	Aluminium Cable Steel Reinforced
OLS	Ordinary Least-Squares
MCDA	Multi-Criteria Decision Analysis
MAWE	Magnitude-Weighted Economic (MCDA)
Notation	Variable Representation
C_{tot}	total initial investment (SPV and GES) (JPY)
$C_{non-loc}$	non-location-dependent costs (SPV-GES) (JPY)
C_{loc}	location-dependent costs (SPV-GES) (JPY)
C_{trans}	transmission costs (SPV and GES) (JPY)
C_{land}	land costs (SPV and GES) (JPY)
C_{exc}	drilling/excavation costs (GES) (JPY)
C_{sc}	supply chain costs (SPV and GES) (JPY)
c_{ckt-km}	transmission cost per km of circuit (JPY/km)
L_{min}	horizontal distance to nearest substation (km)
P_{peak}	peak capacity of SPV plant (MW)
P_{GES}	peak capacity of required GES (MW)
R	resistance per km of transmission line (Ω/km)
D_{CBD}	distance from CBD (km)
D_{manu}	distance from the material manufacturing site to FP (km)
D_{msc}	distance from the nearest FP to the k-means MP (km)
F_L	freight load of the material to be transported (tons/MW)
c_{ft-km}	cost of transporting one ton load for one km (JPY/km-ton)
$C_{road-km}$	per km cost of road construction (JPY/km)

Table 1. Cont.

Notation	Variable Representation
C_{exc}	unit cost of excavating (JPY/m ³)
V_{exc}	excavation volume (m ³)
C_{sys}	system cost for the SPV-GES (JPY)
$C_{planning\&approval}$	planning and permitting costs (SPV and GES) (JPY)
S_{out}	annual maximum energy output of the system (MWh)
CF	capacity factor
A_t	annual maintenance and operation (O&M) cost (JPY/year)
t	lifetime of the SPV-GES plant (years)
k	curtailment ratio

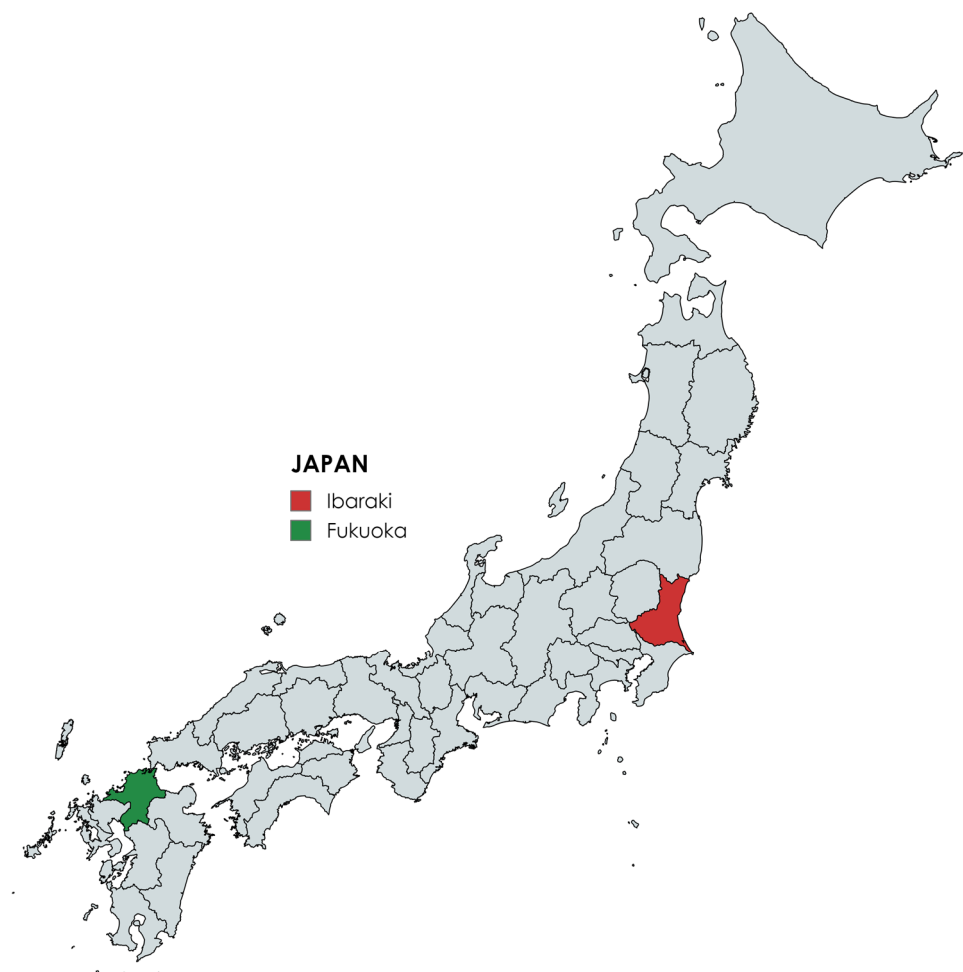


Figure 1. Fukuoka and Ibaraki locations on the map of Japan.

2. Materials and Methods

2.1. Maps and Description of Simulation Areas

To test the hypothesis of GES cost variability in curtailment-prone suburban areas, regions of 50×50 km² were selected in a mostly mountainous suburban area of the Fukuoka metropolitan area and a flat suburban area of Ibaraki near the Tokyo metropolitan area. According to the variations in land, transmission and supply chain costs in existing case studies [10,41], it is assumed that the SPV-GES location-dependent costs can be optimized reasonably within the 2500 km² area.

Fukuoka in the Kyushu region has increasing SPV installations due to the abundant solar radiation [42], which leads to high curtailment due to oversupply and isolation of the Kyushu grid [12,43]. The city of Fukuoka is a commercial center of the Kyushu region. Utility-scale storage is thus an immediate requirement in Fukuoka in order for the SPV LCOE to be lower than that of fossil fuel generation [12,14]. The simulation area in Fukuoka is to the southeast of the city. Most of this area is mountainous and includes parts of Oita and Kumamoto Prefectures as well. This area is shown in Figure 2. It can be seen that most of the target area in Fukuoka is mountainous. However, due to the suburban area being non-contiguous, flat areas were designated as flat points (FPs), which were assumed to be circular zones with 3 km radii. The Central Business District (CBD) was designated as Fukuoka City Hall, which is in the vicinity of the commercial city center (Figure 2). The Fukuoka Cargo Terminal Station was assumed to be the origin of the material supply point for SPV-GES infrastructure, designated as the Load Distribution Center (LDC) (Figure 2). The manufacturing bases of GES and SPV were denoted as “Manu(GES)” and “Manu(SPV)”, respectively, and were based on actual factory locations outside the simulation area (Figure 2). A concrete manufacturing plant of Yamau Corporation was assumed to be the GES supply source and a semiconductor manufacturing plant of Tokyo Electron Kyushu Limited was assumed to be the SPV cell supply source [44]. The distance from these manufacturing sites to each plant location was used to calculate supply chain costs. Three actual substations in the area were marked to serve as the interconnection points for the SPV-GES hybrid plant [43] (Figure 2). Table 1 lists the marked points within the Fukuoka and Ibaraki simulation areas.

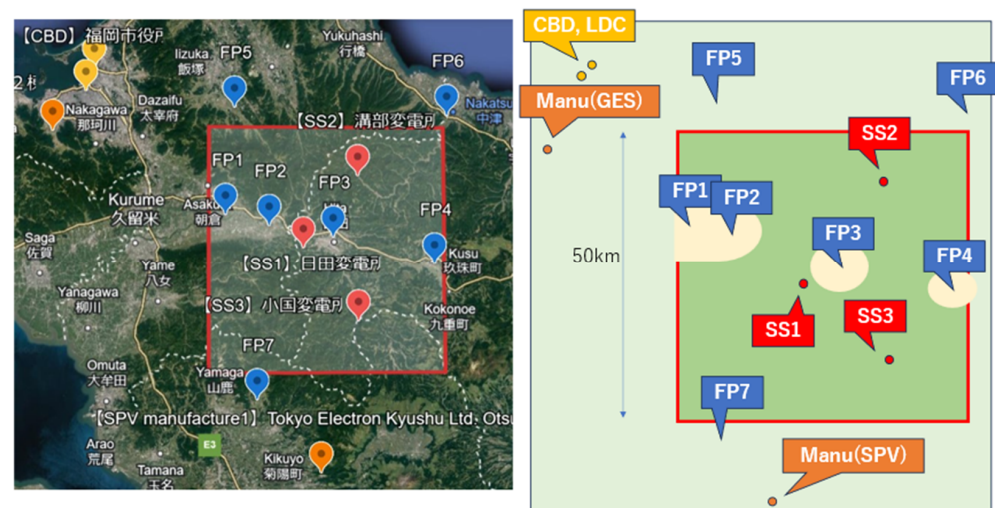


Figure 2. The 2500 km² simulation area in the Fukuoka case (red square in left pane), with assumed points. (Note: The Japanese names of the places are unchanged).

Ibaraki Prefecture is in the Kanto plain, one of the largest flatland areas in Japan. It is located in the Tokyo metropolitan area, and serves as a key suburban outskirts of Tokyo. Figure 3 shows the simulation area for Ibaraki. In contrast to the Fukuoka case, most of the 2500 km² area is flat with few mountainous areas, while no FPs are established in Figure 3 and three mountain points (MPs) are set up, which is the reverse of an FP with an assumed 3 km radius mountainous terrain area. This simulation area was chosen in Ibaraki as it is sandwiched between Kasumigaura, the second largest lake in Japan, in the east, and the Abukuma highlands in the north. The rest of the Tokyo metropolitan area is too densely populated for utility-scale power plants [45]. As in Fukuoka, three substations (SS); material manufacturing bases, Manu(GES) and Manu(SPV); a Central Business District (CBD); and a Load Distribution Center (LDC) are denoted for Ibaraki in Figure 3. The CBD is located in Shinjuku Ward, Tokyo, which is the biggest commercial center of Tokyo, and the LDC is the Tokyo Cargo Terminal Station located in Shinagawa Ward. In the Ibaraki case, Manu(GES) is a concrete product manufacturing plant of the

Sanyo Remicon Corporation, and Manu(SPV) is a solar cell manufacturing factory of the Panasonic SPT Corporation [46].

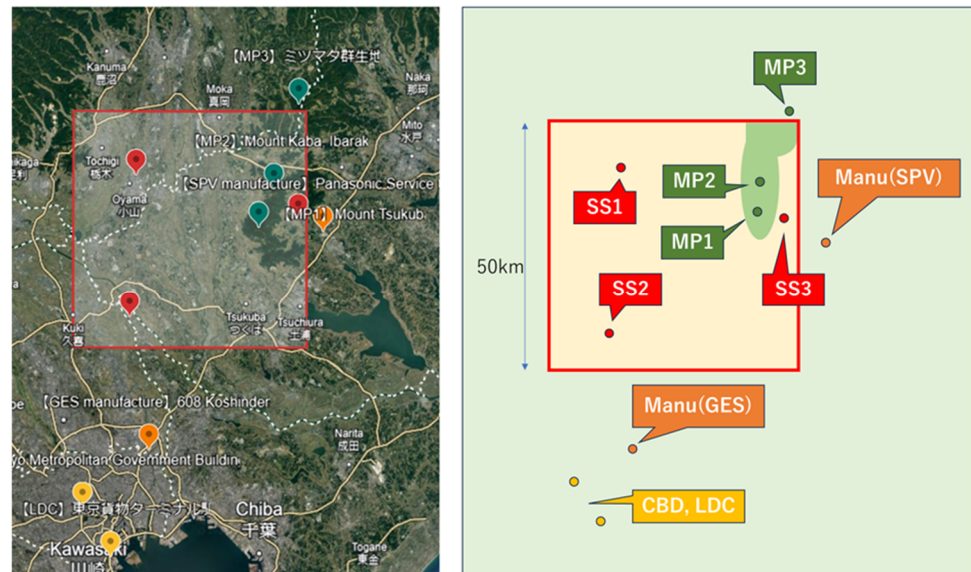


Figure 3. The 2500 km² simulation area in the Ibaraki case (red square in left pane), with assumed points. (Note: The Japanese names of the places are unchanged).

2.2. GES System Description

In this study, a piston-type GES (P-GES) with high geographical applicability and modularity was employed to analyze the variation in GES installation costs in the two 2500 km² areas. P-GES can be constructed in a variety of terrains, including flat and mountainous areas [21,25,28]. Moreover, the P-GES design and construction process is standardized, making it easy to replicate and expand [28]. Another major advantage of the P-GES is its hydraulic system, which allows for a rapid response of typically seconds, which enables voltage and frequency adjustment and provision of reserve services [20,28]. Although frictional losses are higher than in other GES, innovative solutions are being researched, such as rolling membranes, to improve efficiency [23,47] and designs to withstand subsurface pressure and water flow [21]. Figure 4 shows an overview of the P-GES system, where the piston in the vessel moves up and down repeatedly to store and release energy through the conversion of potential energy and electric power. Table 2 shows the assumed GES system parameters for this study required for a 4 Mwh/1 MW P-GES system. Steel and reinforced concrete have been identified as excellent GES plant construction materials in terms of durability, density and material cost [24]. In this study, it was assumed that reinforced concrete is used for the container structure and steel for the piston structure.

Table 2. Parameters of the P-GES system for 1 MW.

Parameter (m)	Container	Piston	Return Pipe
Height	137.64	68.82	137.64
Diameter	8	8	0.12
Thickness	2.09	-	0.014

The above parameters were derived from the following set of equations, which was also used to evaluate the LCOS of the GES system within the hybrid SPV-GES plant. The energy storage capacity of the P-GES can be expressed as in Equation (1), as discussed in the previous literature [21,24,28,47].

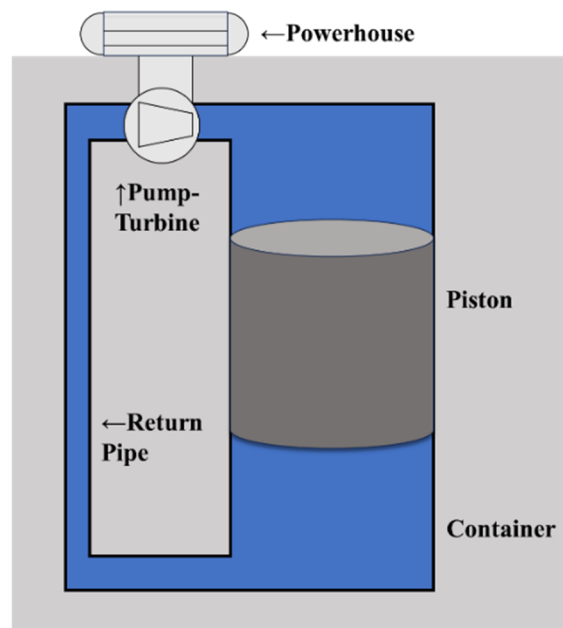


Figure 4. P-GES system of 1 MW assumed for this study.

$$E = (\rho_p - \rho_w) \left(\frac{1}{4} \pi D^2 h \right) g z \mu \quad (1)$$

where E is the stored energy production (J), g is the gravitational acceleration (m/s^2), z is the height of the water (m) and μ is the storage efficiency. For the mechanical system, p (density of the piston), r_w (density of the water), D (container/piston diameter) and h (height of the piston) can be used instead of the mass of the piston. The higher the piston height h , the greater the energy production. The energy production will be greater. However, this leads to a decrease in water depth z . The optimal piston height is determined by solving for the critical point in Equation (2).

$$\frac{\delta E}{\delta h} = 0 \quad (2)$$

Therefore, when $h = z$, the energy production of the storage system is at the maximum. Hence, the optimal piston height is half the height of the container. In order to withstand the load pressure on the container, the walls of the system must have an appropriate thickness. The thickness of the container (t) is related to the stresses in the concrete σ_{st} which is identified from [21], and can be written as in Equation (3).

$$\sigma_{st} = \frac{H_t}{1000t + (m - 1)A_{st}} \quad (3)$$

where H_t represents the maximum hoop tensile force acting on the vertical segment of the circular wall, m is the module ratio and A_{st} is the area of rebar used as reinforcement in the structure. These parameters are obtained from Equations (4)–(6).

$$H_t = \frac{(\rho_p g + w - k_0 y) H D}{2} \quad (4)$$

$$m = \frac{280}{\sigma_{cbc}} \quad (5)$$

$$A_{st} = \frac{H_t}{\sigma_{st}} \quad (6)$$

where σ_{cbc} is the compressive stress in the concrete, w is the specific gravity of water, k_0 is the coefficient of soil pressure at rest and γ is the weight of the soil (kg/m^3). With the parameters of Table 2 for the thickness pipe and efficiency 0.8, we arrived at a GES capacity of 4 Mwh/1 MW. These parameters were used to calculate the LCOS for the P-GES.

2.3. Location-Dependent Cost Parameters

The focus of this study is to introduce a model that can optimize the location-dependent costs for a hybrid SPV-GES system in suburban areas. The model aims to identify the geographic points where the costs of installing the SPV-GES hybrid system are minimized at a certain location in the suburban areas. The model is based on the MUFSP model introduced by [10] in their study of suburban SPV plant cost optimization. However, several additional parameters are considered due to the nature of GES systems being completely different from SPV plants. The total cost function of an SPV-GES hybrid system can be expressed as in Equation (7).

$$C_{tot}(x) = C_{loc}(x) + C_{non-loc} \quad (7)$$

where C_{tot} is the total initial investment divided into C_{loc} (location-dependent variable costs) and $C_{non-loc}$ (non-location dependent fixed costs) within the simulation area. x represents the socioeconomic factors affecting C_{loc} .

The 2500 km^2 simulation areas shown in Figures 2 and 3 were divided into 500×500 meshes, and converted to 500×500 matrixes in a MATLAB SIMULINK R2023a environment. (Note that each mesh element has a geographic resolution of 100 m^2 .) As shown in Figure 5, each of the 250,000 elements in the 500×500 matrix was integrated with GIS functions and various socioeconomic, technological and geographic data to determine the C_{loc} variation for the SPV-GES plant in a suburban area. In other words, each matrix element contains a corresponding C_{loc} value. Equation (8) below represents the objective function and focuses on transmission, land, supply chain and excavation costs.

$$C_{loc}(x) = C_{trans}(x) + C_{land}(x) + C_{sc}(x) + C_{exc}(x) \quad (8)$$

where C_{trans} represents transmission costs, C_{land} represents land costs, C_{sc} represents supply chain costs and C_{exc} represents drilling costs. C_{exc} is specifically for P-GES installation, while the other cost functions are associated with both SPV and GES installations. This equation's minimization at a specific point in the simulation areas will reflect the acceptance or rejection of this study's hypothesis that SPV-GES hybrid system costs are variable in suburban areas and can be minimized at a particular mesh element.

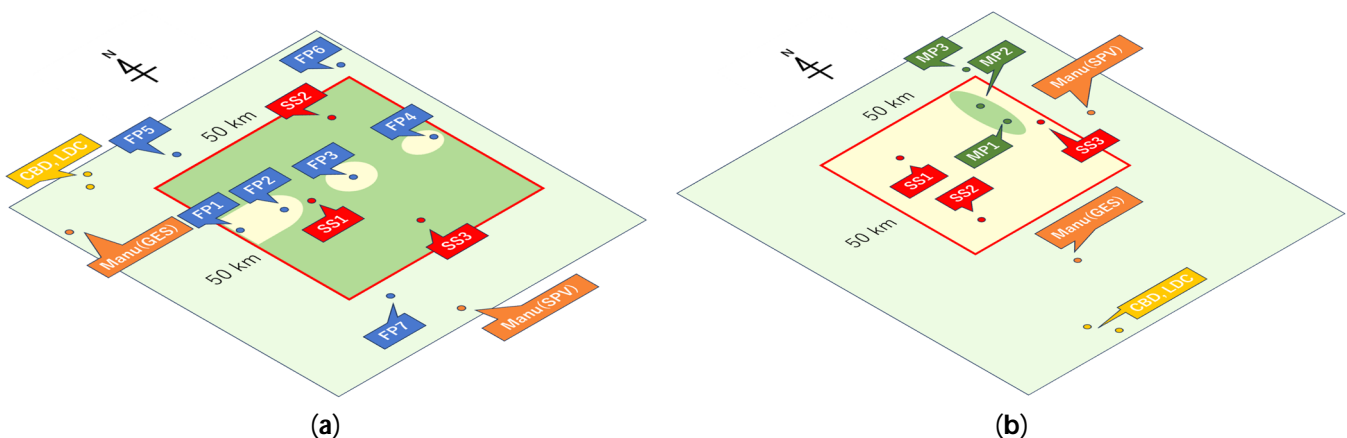


Figure 5. Orientation of the simulation areas of (a) Fukuoka and (b) Ibaraki for the projection of the 3D visualization of location-dependent costs for the SPV-GES hybrid system.

2.3.1. Transmission Costs

The transmission cost function consists of the various costs required to connect a power source to a substation, including conductors, labor costs, grid upgrades, land use costs, and taxes associated with those costs. The Ministry of Land, Infrastructure, Transport and Tourism reports that the construction cost per km of 66 kV transmission line in Japan is typically JPY 35 million [48]. Equation (9) is the transmission cost function for each element of the matrix C_{loc} .

$$C_{trans}(x) = c_{ckt-km} \cdot L_{min} \quad (9)$$

where C_{ckt-km} is the transmission cost per km of circuit (JPY/km) and L_{min} is the horizontal distance from each simulation point to the nearest substation (km). As shown in Figures 2 and 3, all 500×500 simulation points in the Fukuoka and Ibaraki simulation areas are connected to the closest of the three substations (SS1-3) in the respective areas.

In addition, the peak capacity of the SPV installation centered at each point in the simulation area is affected by the rated voltage and characteristics of the transmission line; an aluminum cable steel-reinforced (ACSR) conductor was considered for the 66 kV transmission line. The resistance and the length of the transmission line were used to calculate the peak capacity in Equation (10) at each simulation point.

$$P_{peak}(x) = \frac{(66 \text{ kV})^2}{2(R \cdot L_{min}(x))} \quad (10)$$

where P_{peak} is the peak capacity (MW) of the SPV plant at each simulation point, which is the rated output of the SPV installation and R is the resistance per km of transmission line (Ω/km), which is 0.262 (Ω/km) (Transmission Cables in Japan: https://www.hst-cable.co.jp/products/pdf/cableg3_2.pdf, accessed on 24 March 2024). The capacity determination equation for a GES system is discussed in Section 2.4. The transmission loss for special high-voltage transmission lines above 7 kV was 1.3% for FY 2018 and 2019 in the Kyushu region, so transmission losses were neglected in this study [43].

2.3.2. Land Costs

The land cost functions are based on the existing MUFSP model [10], where the distance to the CBD was proven to be the most critical factor determining land cost in a suburban area, which resonates with previous studies as well [34,35]. The cost function is guided by the principles of hedonic pricing, where a least-squares (OLS) regression model for determining property and land prices is used. The distances from the CBD and LDC in Table 2 are considered as the determining factors for C_{land} in both Fukuoka and Ibaraki. In the Fukuoka area, the three variables are the distance from the CBD, LDC and 2nd CBD, where the 2nd CBD is the center of Kurume City in Fukuoka Prefecture, a populated city near this area. In the Ibaraki area, six variables are introduced: the CBD, LDC, 2nd CBD, 3rd CBD, 4th CBD and 5th CBD, where the 2nd~5th CBDs are Saitama City, Utsunomiya City, Mito City and Tsukuba City, respectively. This is an improvement over existing models, since the CBDs in Japanese developed cities are located close to each other, influencing land prices in a complex way. Equation (11) below represents the hedonic land cost function.

$$\ln(C_{land}) = \left(\beta_0 + \sum_{i=1}^n \beta_i X_i + \varepsilon_0 \right) \quad (11)$$

where C_{land} is the land price public notice data integrated in GIS (QGIS Desktop 3.32.1) for Fukuoka (934 samples) and Ibaraki (351 samples) in the target area [49]. β_0 is the intercept, β_i is the regression coefficient on and ε_0 is the standard error of the regression. The per MW land requirement of SPV installation is given in [50], whereas for GES it is 256 m^2 , as stated in [21].

Tables 3 and 4 give the regression coefficients for Fukuoka and Ibaraki, respectively. In the case of Fukuoka, both the CBDs are statistically significant in contributing to the land price, while in the case of Ibaraki all the CBDs, except for CBD 3, are statistically significant. This has interesting implications for any suburban construction activity, since multiple policies impact the land price determination in Japanese suburban areas.

Table 3. Land cost regression results for Fukuoka.

Variables	Reg. Coefficient	Standard Error	p-Value
Intercept	12.392	0.0921	0.0000
Distance from CBD (X_1)	0.108	0.0400	0.0068
Distance from LDC (X_2)	−0.136	0.0367	0.0002
Distance from 2nd CBD (X_3)	−0.00128	0.0056	0.0819
R-Square: 0.88			
N = 934			

Table 4. Land cost regression results for Ibaraki.

Variables	Reg. Coefficient	Standard Error	p-Value
Intercept	8.857	2.0512	0.0000
Distance from CBD (X_1)	2.729	0.589	0.0000
Distance from LDC (X_2)	−1.812	0.399	0.0000
Distance from 2nd CBD (X_3)	−0.895	0.201	0.0000
Distance from 3rd CBD (X_4)	−0.020	0.0135	0.1402
Distance from 4th CBD (X_5)	0.0952	0.133	0.0000
Distance from 5th CBD (X_6)	−0.0442	0.0121	0.0003
R-Square: 0.55			
N = 351			

2.3.3. Supply Chain Costs

In the modeling, GES plant materials such as power houses, pumps and turbines, containers and other structures, and SPV equipment such as solar modules, inverters and mounting structures, were assumed to be locally manufactured and transported by truck. This is because Japan promotes domestic manufacturing for VRE infrastructure [39,46]. The details of Manu(SPV) and Manu(GES) (assumed manufacturing locations for GES and SPV infrastructure) are given in Figures 2 and 3.

One key contribution of this study was to express the C_{sc} in a novel way to account for suburban mountainous terrain. Firstly, the differences in transportation between plain and mountainous areas are considered. The Fukuoka simulation area is mostly mountainous, as shown in Figure 2, while the Ibaraki simulation area is mostly flat, as shown in Figure 3. It is assumed that, to transport materials to each simulation point, where road networks are not developed, transportation roads must be constructed (this is discussed in [51], where mountain-slope SPV construction was considered a constant when accounting for supply chain costs). The supply chain process begins by transporting materials from the material manufacturing plant to the nearest flatland point to each simulation point (x), and from there new road construction costs are considered for mountainous areas. The k-nearest neighbor points were obtained, using the k-nearest clustering method [52], for estimating the mountainous terrain in the GIS interface. In the Ibaraki case, where most of the area is level, the cost term for new road construction is not considered since mountainous points would be ignored for an optimized location.

A second consideration is that the bird's-eye shortest distance between manufacturing plants (Manu) to each simulation point has to be converted to road distances. A coefficient of Distance-to-Road (DtoR) with a value of 2.05 is assumed in the Fukuoka case and 1.58 in the Ibaraki case. This is based on the average of a ratio of road distance to horizontal distance calculated using Google Earth GIS data for the four sides of each $50 \times 50 \text{ km}^2$ simulation area. Taking these into account, the supply chain cost C_{sc} for SPV installations for the Fukuoka case is shown in Equation (12) and for the Ibaraki case in Equation (13).

$$C_{sc}(x) = P_{peak} \cdot F_L \cdot \left[c_{ft-km} \cdot 2.05 (D_{manu} + D_{msc}) \right] + c_{road-km} \cdot \max[D_{msc} - 3, 0] \quad (12)$$

$$C_{sc}(x) = P_{peak} \cdot F_L \cdot \left[c_{ft-km} \cdot 1.58 (D_{manu}) \right] \quad (13)$$

where C_{sc} is the total supply chain cost at each simulation point in the area according to the peak capacity P_{peak} (in JPY), F_L (tons/MW) is the freight load of the material to be transported (50,720 metric tons/MW for GES [22] and 105.8 metric tons/MW for SPV [53]), D_{manu} is the distance from the material manufacturing site to the nearest flat point at point (FP) (in km), D_{msc} is the distance from the nearest FP to the k-means mountainous area (in km), c_{ft-km} is the cost of transporting one ton load for 1 km by truck (15.95 (Ministry of Land, Infrastructure, Transport and Tourism: Standard Freight Rates for General Cargo Trucking Business: <https://www.mlit.go.jp/en/road/index.html> (accessed on 24 March 2024)) JPY/km-t) and $c_{road-km}$ is the per km cost of road construction for each k-means mountainous simulation mesh point (85,000,000 (Ministry of Land, Infrastructure, Transport and Tourism: Estimation Methodology for Each Renewable Energy Type <https://www.mlit.go.jp/en/tec/index.html> (accessed on 24 March 2024)) JPY/km). These equations are a significant improvement over [51], which only assumed constants for mountainous SPV supply chain costs. Equations (12) and (13) also add to the existing MUFSP model [10] for considering mountainous suburban areas. For GES, the P_{peak} term is replaced with demand-adjusted GES capacities.

2.3.4. Excavation Costs

This cost factor is exclusive to GES, since SPV installations do not require any excavation. Installation of a GES plant requires $22,410 \text{ m}^3$ of excavation per MW according to the design in Section 2.1 [21,22]. Excavation costs vary from one GES plant installation site to another depending on geographical factors such as geology and technical factors such as technology [28]. In this study, two types of excavation costs (JPY/ m^3) were used to distinguish between excavation costs in mountainous and flat areas. Data from the metropolitan area outer discharge channel were used for excavation costs in flat areas (1882 (The Metropolitan Area Outer Underground Discharge Channel: https://www.ktr.mlit.go.jp/ktr_content/content/000053312.pdf (accessed on 24 March 2024))), while data from the Shiosaka tunnel construction in Nagano Prefecture, a mountainous area, were cited for excavation costs in mountainous areas (1441 (Shiozaka tunnel: https://www.pref.nagano.lg.jp/omachiken/nyusatsu/documents/uchu2tn_keiyaku.pdf (accessed on 24 March 2024))). The values obtained from these data indicate that excavation costs in flat areas are higher than those in mountainous areas. The excavation cost function is shown in Equation (14).

$$C_{exc}(x) = c_{exc} \cdot V_{exc} \quad (14)$$

where c_{exc} is the unit cost of excavating at each simulation mesh point (JPY/ m^3) and V_{exc} is the excavation volume (m^3). This equation provides the second methodological advancement of the MUFSP model [10] after C_{sc} .

2.4. Hybrid SPV-GES Concept and LCOE/LCOS Evaluation

The reason for co-locating the SPV-GES hybrid system is to reduce costs. First, unlike the case where transmission lines are installed at separate locations for each plant, only one transmission line is needed for the integrated plant, which reduces transmission costs. In

addition, land costs for GES can be negligible to the larger area of SPV, making approval costs simultaneous. In terms of supply chain costs, the construction of a new road in the mountainous area is necessary, but if both plants are constructed at the same site, only one road line is needed, thus reducing the cost of new road construction. For the LCOE calculations described below, none of the location-independent costs are affected by co-locating the SPV and the GES plants. The same construction, labor, and administrative costs are assumed as if they were built at different locations. The LCOE is estimated using Equation (15).

$$LCOE = \frac{C_{tot} + \sum_{t=1}^{t=n} \frac{A_t}{(1+i)^t}}{\sum_{t=1}^{t=n} \frac{S_{out} \times CF}{(1+i)^t}} \quad (15)$$

where t is a year time-step, n is the lifetime period of the SPV-GES system, C_{tot} is the system capital cost from Equation (7), A_t is the annual maintenance and operation (O&M) cost of the system, S_{out} is the annual maximum energy output of the system and CF is the capacity factor affected by curtailment and i is the discount rate. The location-independent cost for both SPV and GES plants is expressed by Equation (16).

$$C_{non-loc} = C_{sys} + C_{planning\&approval} \quad (16)$$

where C_{sys} is the system cost for the SPV-GES plants, including the cost of materials and modules and the construction cost [44]. The system cost for GES is based on a P-GES plant of similar design multiplied by CF [21]. $C_{planning\&approval}$ includes site evaluation, planning and permitting costs, project management and development costs, and is assumed to be 5% of the system cost, based on similar projects [54]. For the annual system cost A_t , energy storage systems require regular maintenance, which was assumed to be 5% of the system cost of GES [21], much more than the SPV O&M costs of 3% [53]. This because the mechanical parts of P-GES require more maintenance, such as lubrication for pumps/turbines and labor cost behind regular repair and maintenance [28]. All the cost factors are listed in Table 5.

Table 5. LCOE/LCOS parameter description and values for the hybrid SPV-GES system.

Coefficient	Meanings	Value	Reference
C_{sys} (JPY/MW)	The system cost of SPV	180,000,000	[44]
	The system cost of GES	185,000,000	[21]
$C_{planning\&approval}$ (JPY)	The cost for planning, approval, and management	5% of the system cost	[54]
$C_{O\&M}$ (JPY)	The annual O&M costs of SPV	3% of the system cost	[53]
	The annual O&M costs of GES	5% of the system cost	[21]
i	Annual discount rate	7%	[53]
n (year)	Life span	30	[50]
k	Curtailment rate of 1 MW SPV	0.2379	[43]

S_{out} (kWh) generated by the plant each year is based on assumptions constructed from Kyushu Electric Power supply data for the year 2022 [43]. First, five days were selected from each of the first, third and fourth quarters along with two days from the second quarter of the year for the output control (MWh) of the SPV in 2022. Then, the maximum load (MW) of the SPV and the demand load (MW) during the same time period were obtained. The average value of the ratio is shown in Equation (17).

$$k = \frac{MW \text{ of Curtailmant}}{MW \text{ of SPV}} \quad (17)$$

The “MW of SPV” is the maximum SPV output for the day (MW), and the “MW of Curtailment” is the output control during the same time period (MW). The calculation results show that $k = 0.2379$. Using this, we can relate the rated output of SPV, P_{peak} , obtained in Equation (10), with the required capacity of GES in the designated simulation mesh point (Equation (18)).

$$P_{GES} = k \cdot P_{peak} \quad (18)$$

where P_{GES} is the maximum required capacity (MW) of GES to utilize the curtailed SPV output. To equally multiply the design of the 1 MW, 4 MWh GES plant in Section 2.1 according to P_{GES} , the storage capacity in a plant with a maximum output of P_{GES} was assumed to be $4 \cdot P_{GES}$ (MWh). This P-GES plant is assumed to operate one cycle per day. The cost and coefficient values are summarized in Table 5.

While $k = 0.2379$ is high compared to the Japanese average of 0.156~0.197 for SPVs above 100 MW [12], solar panel efficiency is estimated to increase with improvement in panel technology. This higher value represents a high-curtailment-zone scenario for a utility-scale GES analysis.

Finally, the discount rate was assumed to be 7% according to average SPV global case studies [33,53]. The lifetime of the SPV-GES system was assumed to be 30 years, based on mega solar plants (>100 MW) [10,50,53]. However, the lifetime of P-GES is estimated to be about 40 years [21,24,28], and some reports suggest that it can be extended to 60 years by developing large capacity P-GES of 1~10 GWh using huge rocks [27,28]. In this study, GES life extent was analyzed till the counterpart SPV was decommissioned.

3. Results

For visualization purposes, Figure 5 shows the orientation of the maps of Figures 2 and 3 for the location-dependent costs' variability representation. The 3D graphs in this section will be projected on the 2D plane of Figure 5a,b in that orientation.

3.1. Location-Dependent GES Cost Variations

Figure 6 shows the results of each location-dependent cost function for GES installation in the Fukuoka area. Figure 7 displays the same for the Ibaraki area. The variations are quite significant in the limited suburban simulation area, which shows the necessity of optimizing the socioeconomic spatial factors if decentralized utility-scale generation is going to be employed in high-curtailment zones. This shows that the first hypothesis of the study can be accepted: *GES installation costs vary significantly in suburban areas affected by the socioeconomics of the city.*

Supply Chain Costs: From Figures 6c and 7c, it is evident that C_{SC} is the most dominant factor of the C_{loc} factors, with an order of magnitude of 10^8 for Fukuoka and 10^7 for Ibaraki. The C_{SC} for Fukuoka is more complicated than Ibaraki, due to the k-means clustering and complex functions involving road constructions in mountainous suburban areas. In the Ibaraki simulation area, based on Equation (13), C_{SC} showed a linear increase with increasing distance from Manu(GES). A significant finding is that supply chain costs alone make suburban, mountainous GES installations economically less feasible. This adds an empirical understanding to the existing economic analyses of GES systems [20,22,23], showing the impact of socioeconomics on GES planning in curtailment-prone areas.

Land and Transmission Costs: C_{trans} was much more significant in both cases (Figures 6a and 7a) with an order of magnitude of 10^7 , one order of magnitude higher than C_{land} (10^6 —Figures 6b and 7b). As Equation (9) shows, the transmission costs are minimal near the three substations in the simulation areas, with higher costs at greater distances from the substations. For land costs, the regression analysis of the hedonic function shows that land prices per unit area increase exponentially toward the significant CBD in the Fukuoka area. The land cost of Ibaraki for GES is quite complex, compared to Fukuoka, due to the effect of multiple CBDs (Figure 7b and Table 4). The previous literature on hedonic land price estimations with single CBDs did not show this effect [10,34]. Even for Chicago, with mul-

multiple CBDs, the Ibaraki nature of the hedonic model was not detected [35]. Thus, this result is significant not only for suburban GES geolocation but also for urban planning policies.

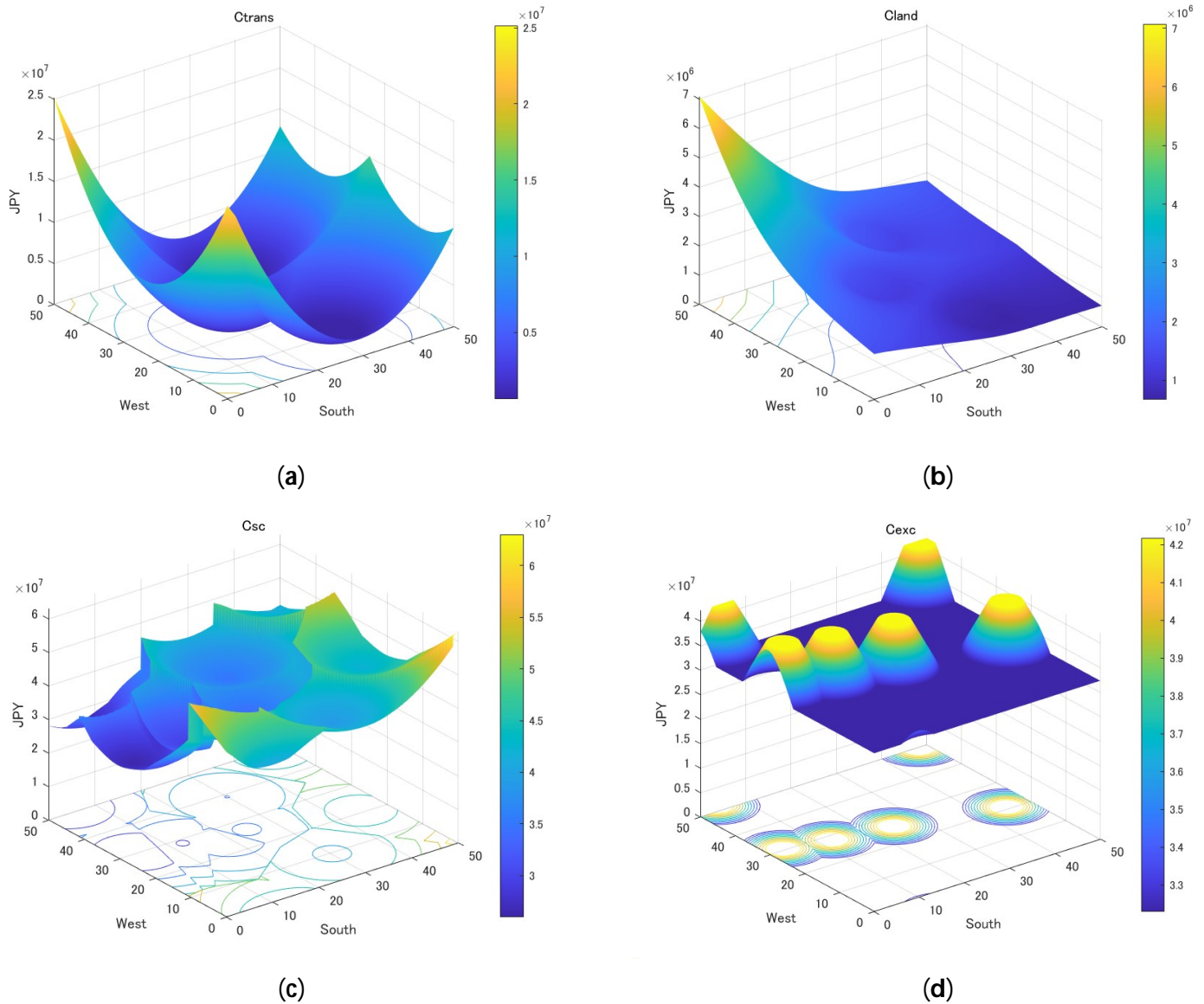


Figure 6. The GES location-dependent cost variations in the 500×500 Fukuoka suburban simulation area for (a) transmission (10^7), (b) land (10^6), (c) supply chain (10^8) and (d) excavation (10^7).

Excavation Costs: These are simple, with binary values, each for flat and mountainous terrains, and a linear increase between the binary levels. The FPs incur higher costs than mountainous regions, as detailed in Equation (14). Albeit binary, this is an important addition to the MUFSP model introduced by [10] due to the order of magnitude of C_{exc} and C_{SC} being comparable. Both the cost functions are inversely related for FPs and MPs, making the optimization of the minimum cost point interesting.

Figure 8 shows the total location-dependent cost (C_{loc}) variations in the Fukuoka and Ibaraki simulation areas for GES. In the case of Fukuoka, the shape of C_{loc} resembles C_{SC} due to the dominance of supply chain costs, as mentioned previously. A closer examination reveals that the edge effects of the total costs are elevated by C_{trans} as we move farther away from the substations. This implies that C_{trans} is the limiting factor of the localization of the minima, as C_{SC} increases with increasing distance from Manu(GES). Since Manu(GES) is in the vicinity of the 1st CBD, it can be said that C_{SC} increases with D_{CBD} . However, C_{trans} radially increases from the epicenter of the SS. As a result, for both cases we see that C_{loc} is

lower when close to the SS and radially increases with the minima point in the vicinity of the SS located closest to the CBD. In Ibaraki case, C_{SC} is linear and more comparable to C_{trans} , with no mountainous terrain, leading to the shape of C_{loc} variation for GES resembling the shape of C_{trans} , but elevated. A well-defined optimized-cost location point exists for GES in both cases, which confirms the second hypothesis of this study, that *suburban location-dependent costs of GES installation can be optimized at a specific location*. This optimized location boils down to the interplay of C_{trans} and C_{SC} , with mountainous areas being out of contention due to elevated C_{SC} . This finding adds to the existing research on GES economics exploration [20,21,25,28] by revealing the impact of geospatial socioeconomics on the CAPEX of suburban GES installation in high-curtailment zones.

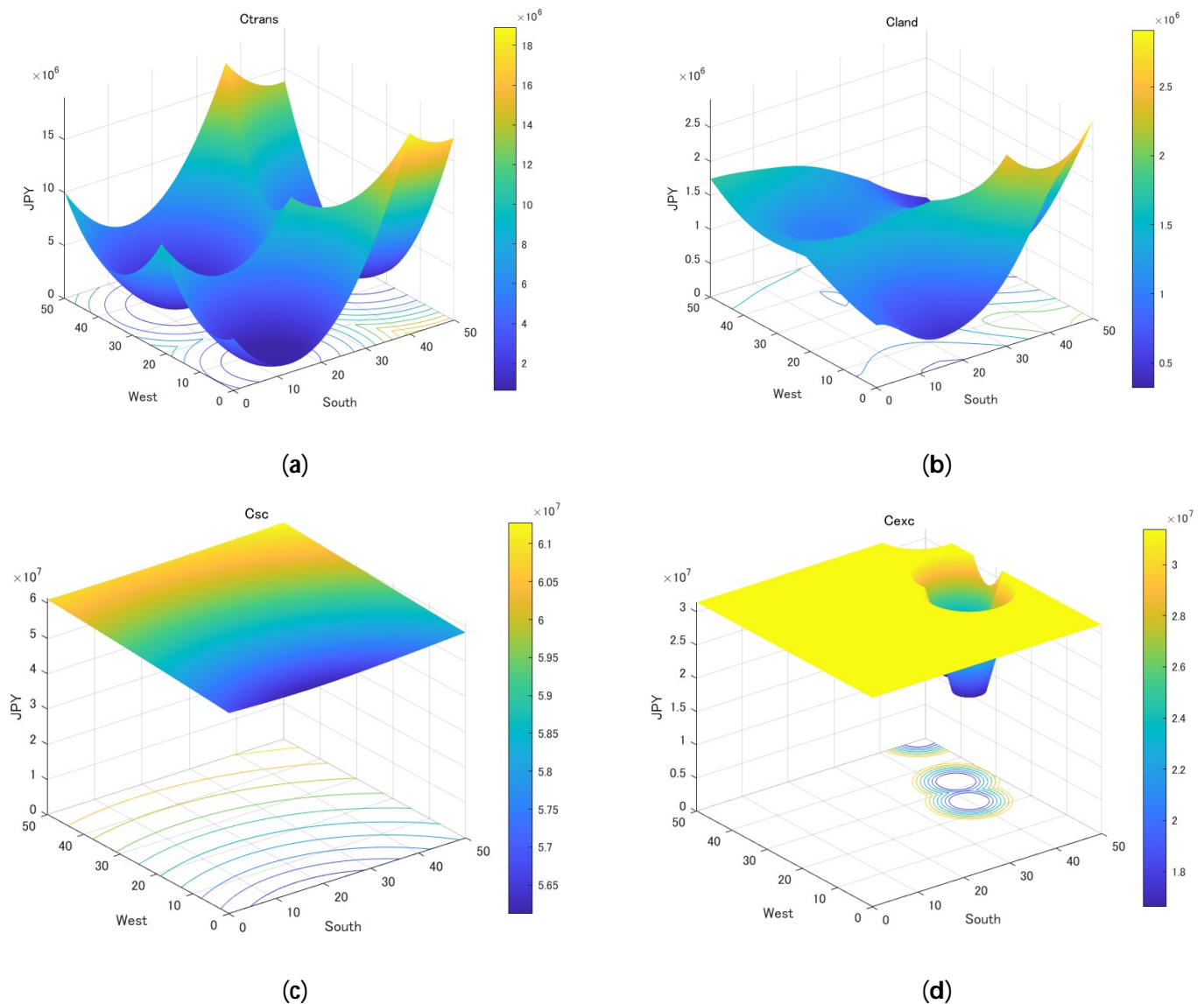


Figure 7. The GES location-dependent cost variations in the 500×500 Ibaraki suburban simulation area for (a) transmission (10^7), (b) land (10^6), (c) supply chain (10^7) and (d) excavation (10^7).

Moreover, when comparing the two regions, it was found that the GES C_{loc} at all of the 500×500 simulation area points of Ibaraki were lower by a factor of at least 0.8 compared to that of Fukuoka (Figure 9). This is specifically due to elevated supply chain costs incurred due to lack of transportation infrastructure in the mountainous areas (Figure 9). Another interesting feature in Figure 9 is that in the Ibaraki case, C_{exc} and C_{SC} are quite comparable to the other cost factors. While [22,25] raised the question of using GES as a curtailment

mitigation storage system, it was not specifically answered. We can infer that suburban metropolitan areas bear a lower cost burden than other suburban areas, making GES a feasible option in curtailment-prone metropolitan grids.

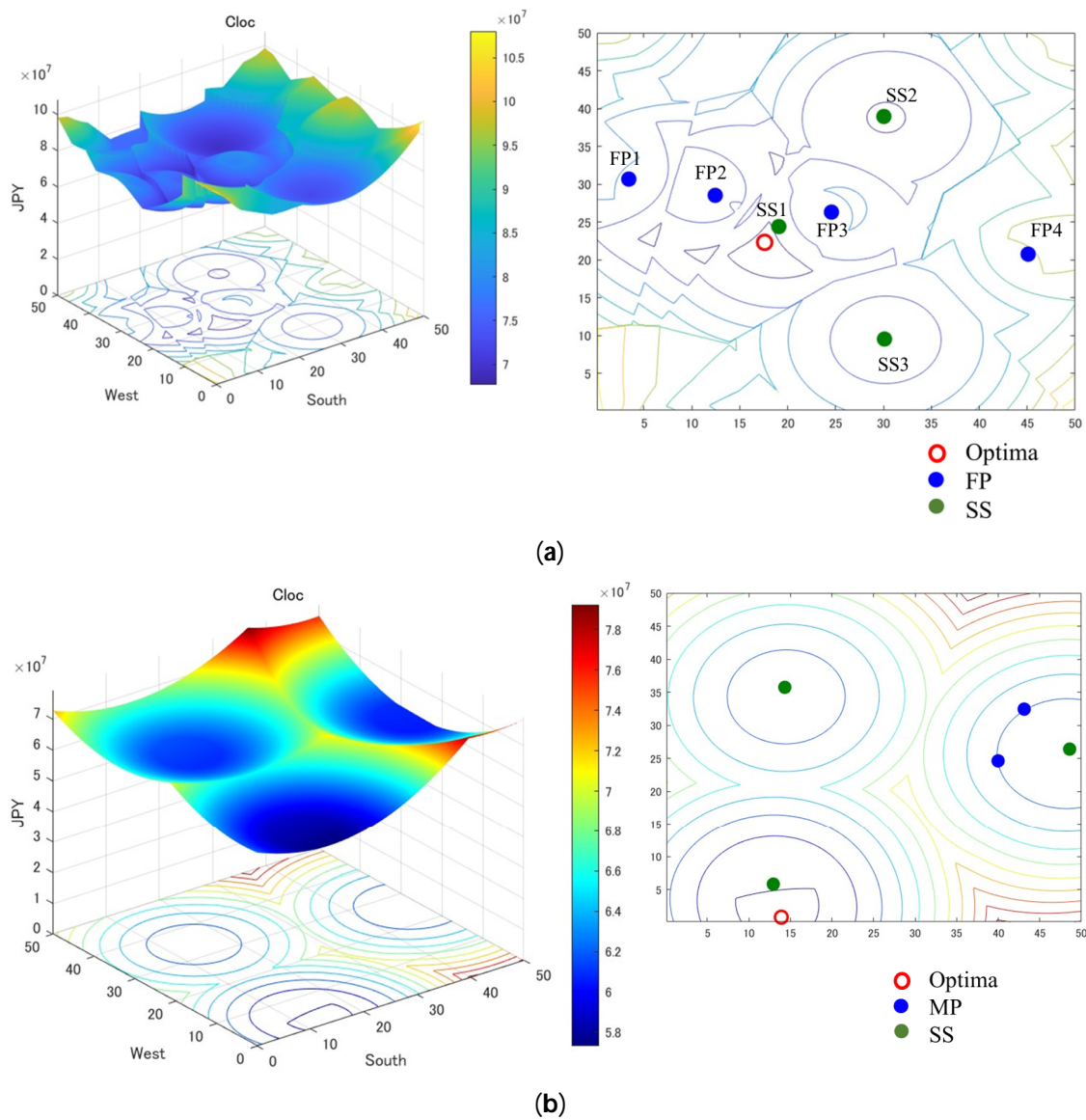


Figure 8. The GES total location-dependent cost variations (C_{loc}) in the 500×500 suburban simulation areas for (a) Fukuoka (10^7) and (b) Ibaraki (10^7).

3.2. Location-Dependent SPV Cost Variations

Figure 10 shows the results of each location-dependent cost function for SPV installation in the Fukuoka area. Figure 11 displays the same for the Ibaraki area. While the nature of C_{trans} and C_{land} for SPV is similar to that of GES in both Fukuoka and Ibaraki, the per MW SPV land cost is two orders of magnitude higher than that of per MW GES, due to the much higher land requirement for SPV than the 256 m^2 per MW for GES [21]. On the other hand, the total weight of materials for SPV is much lesser than GES, making C_{SC} in the SPV cases of the order 10^4 – 10^5 (three orders of magnitude smaller than C_{land}). Thus, land cost becomes the most dominant factor for SPV, as opposed to GES where the supply chain cost was most dominant.

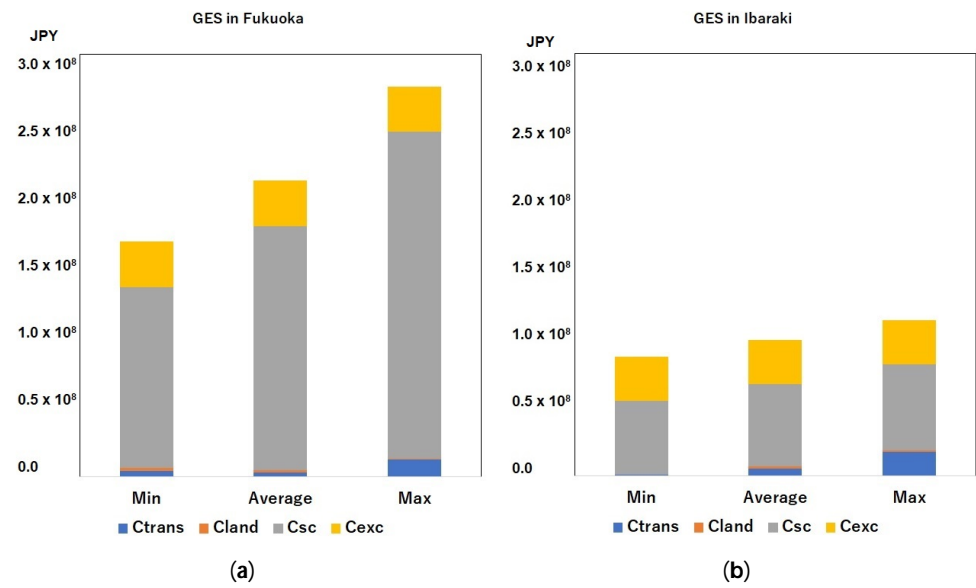


Figure 9. Comparison of the cost factors in C_{loc} for GES in (a) Fukuoka and (b) Ibaraki simulation areas, with the minimum, maximum and average values across the 500×500 simulation area points.

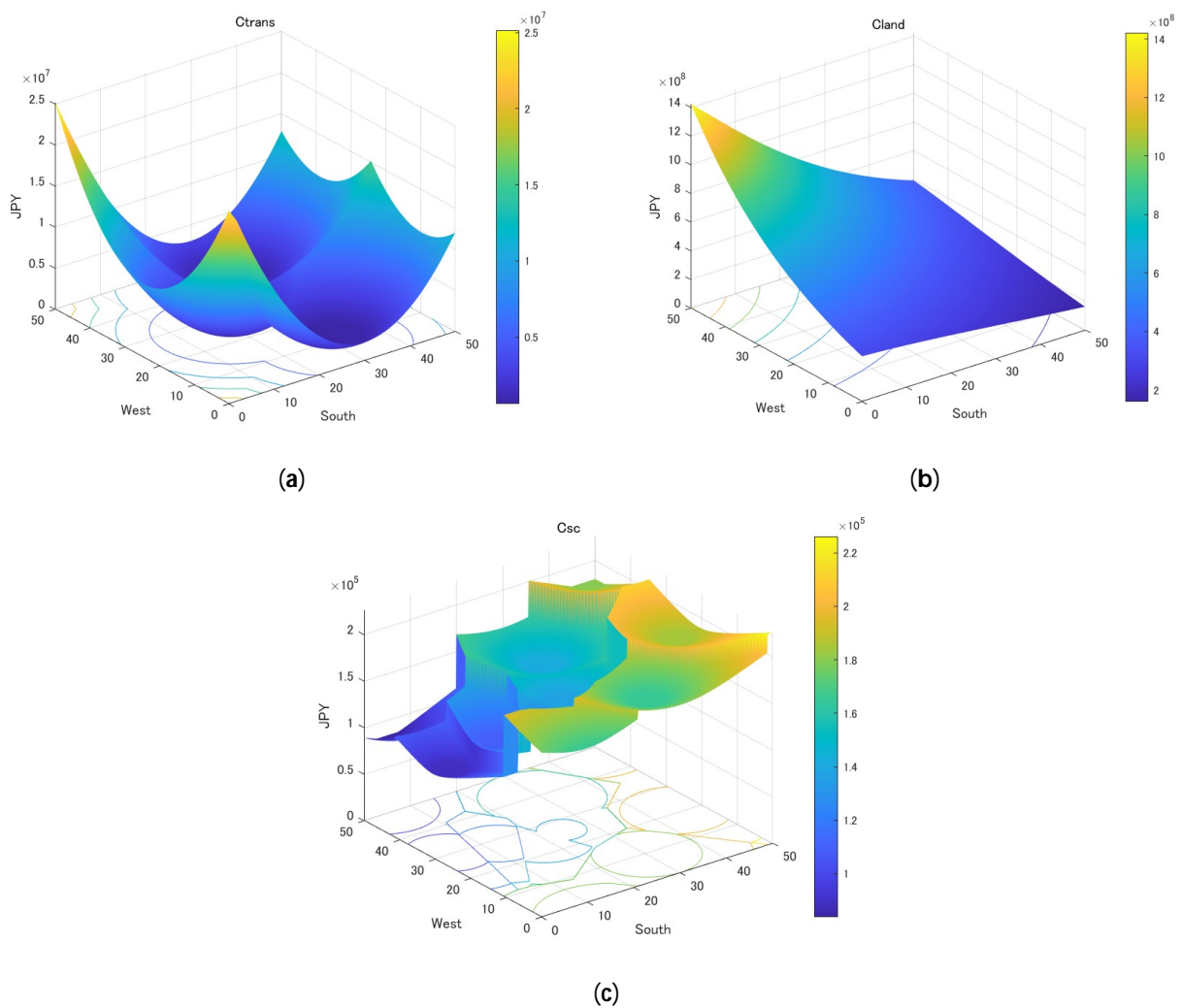


Figure 10. The SPV location-dependent cost variations in the 500×500 Fukuoka suburban simulation area for (a) transmission (10^7), (b) land (10^8) and (c) supply chain (10^5).

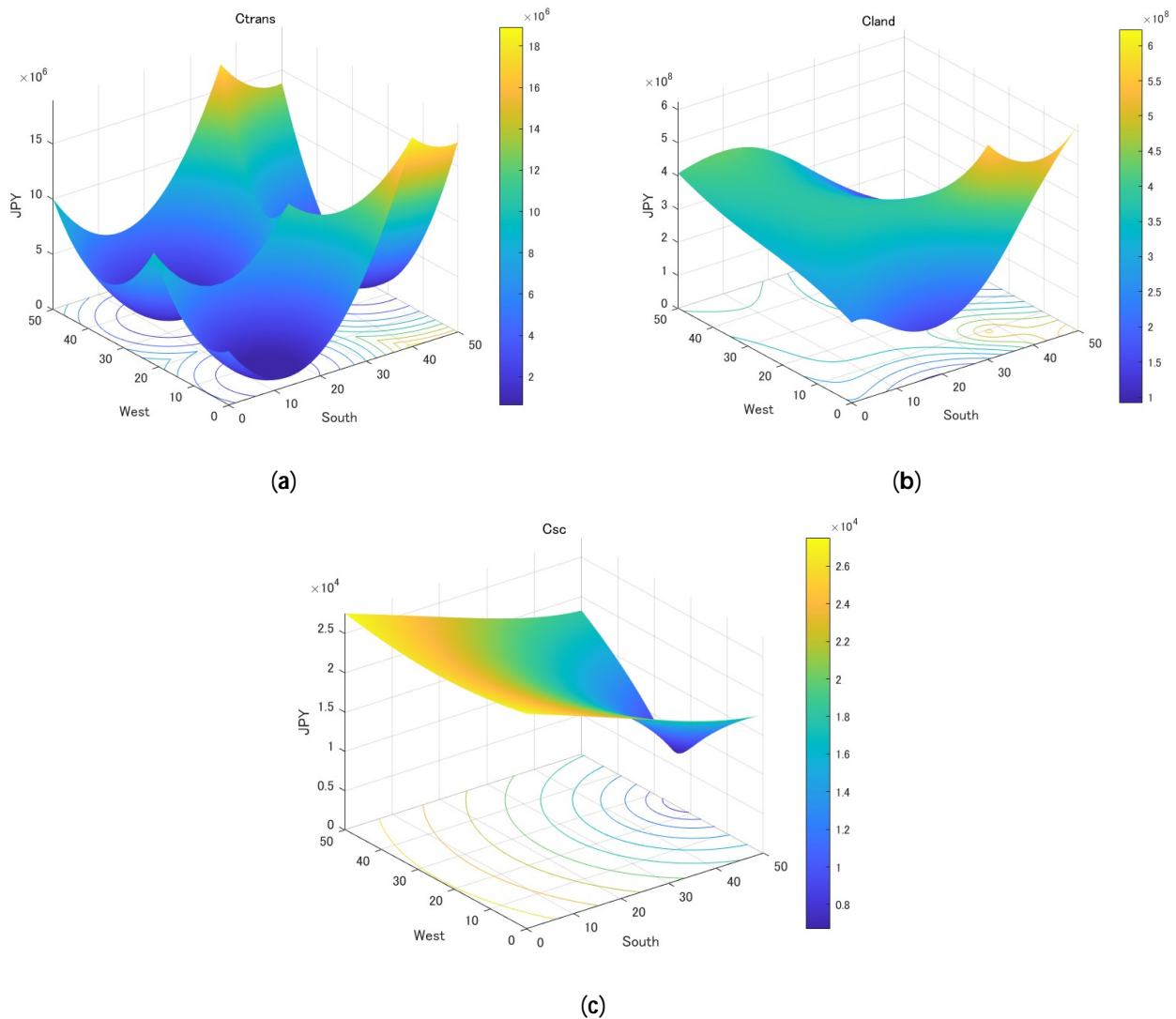


Figure 11. The SPV location-dependent cost variations in the 500×500 Ibaraki suburban simulation area for (a) transmission (10^6), (b) land (10^8) and (c) supply chain (10^4).

Due to the impact of five CBDs, the Ibaraki C_{land} is quite different from the logarithmic variation in Fukuoka. In a sense, C_{land} decreases as we move away from the CBD, while C_{trans} increases radially from substations. Thus, the localization of the minima is an interplay of these two cost factors. Additionally, C_{land} is two orders of magnitude higher than C_{trans} for Ibaraki and one order of magnitude higher in the case of Ibaraki. This is quite different for the MUFSP of Kolkata, India [10], due to the higher land costs in the developed economy of Japan compared to the developing economy of India. This plays a key factor in the optimized cost location, as seen in Figure 12. While in Kolkata, India the C_{loc} for SPV is optimized at a specific location [10], in the developed suburban area of Japan, the optimized-cost location is not that well defined. In general, it would be away from economic centers (CBDs) affected by C_{land} . Moreover, FPs would be the recommended theoretical optimized location than mountainous areas due to higher C_{sc} in mountains. This contradicts the recommendation by [53] which assumed constant C_{sc} for SPV in mountains, proving the advantage of empirically determining location-dependent costs based on the socioeconomics of the installation region.

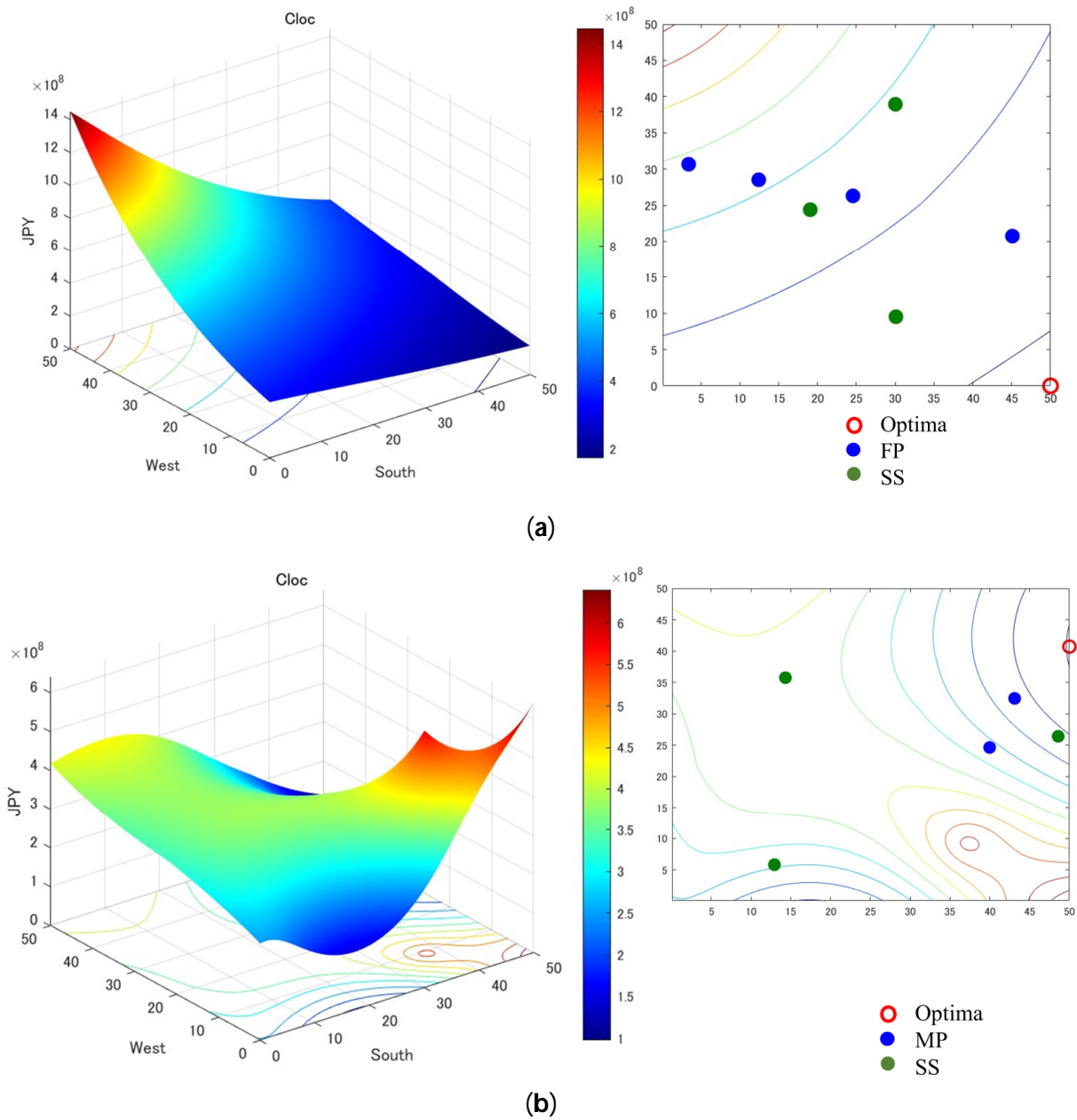


Figure 12. The SPV total location-dependent cost variations (C_{loc}) in the 500×500 suburban simulation areas for (a) Fukuoka (10^8) and (b) Ibaraki (10^8).

Comparing the optimized-cost location for SPV to GES (Figures 8 and 12), GES has defined optima in both Fukuoka and Ibaraki. This is due to the inverse proportionality of C_{trans} and C_{SC} for GES and their comparable orders of magnitude (Figure 9), as opposed to that of C_{land} dominance in case of SPV geolocation (Figure 13). This is further proven by the fact that when we look at Figure 13, in both Fukuoka and Ibaraki, C_{land} is much more dominant than any other cost factor at the minima, averaged and maxima locations within the simulation areas. Thus, in developed nations, social factors and socioeconomics affect the location-dependent CAPEX of storage systems much more than the CAPEX of VREs. This is a counterintuitive result, since it would be assumed that urban socioeconomics would affect hybrid systems similarly. Moreover, it is in developed nations that hybrid systems should be dispatched due to increasing curtailment in decentralized VRE installations. This is another significant finding that provides an answer raised by [21] for further analyzing GES economic feasibility with regard to adoption and installation.

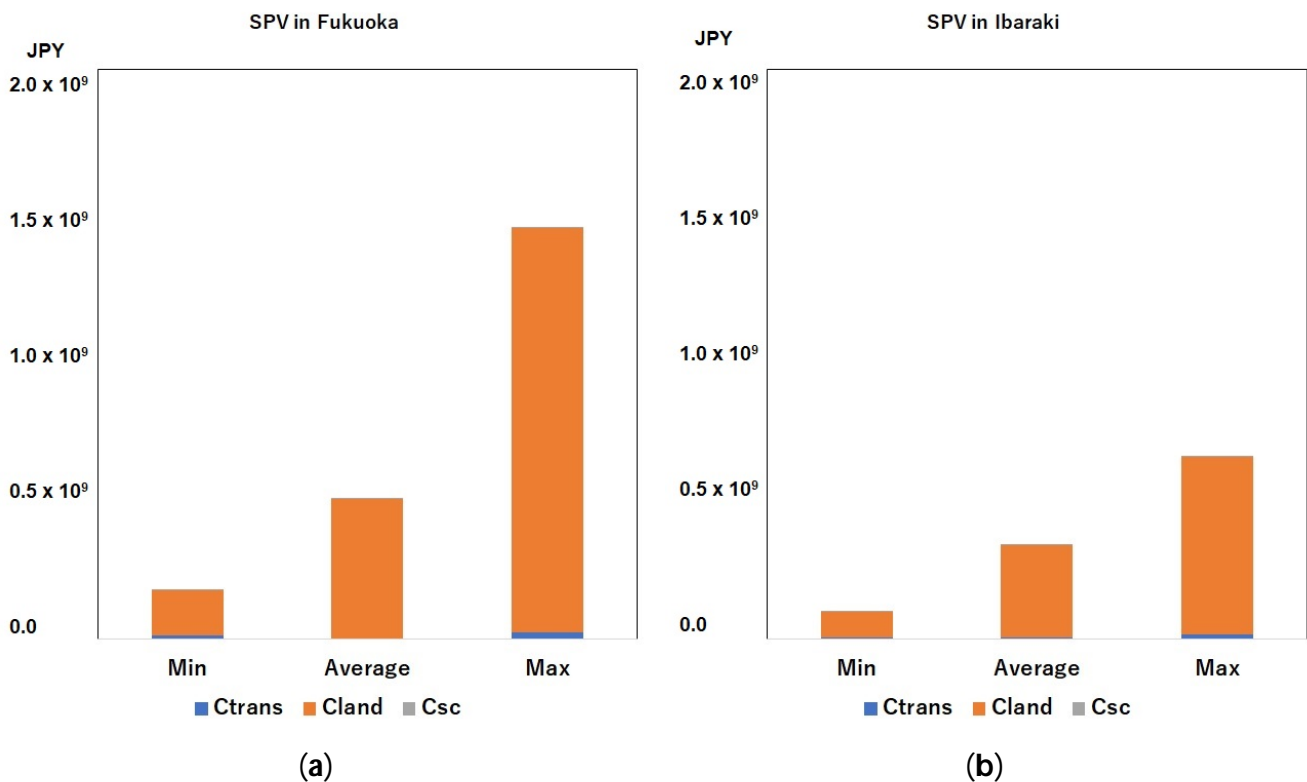


Figure 13. Comparison of the cost factors in C_{loc} for SPV in (a) Fukuoka and (b) Ibaraki simulation areas, with the minimum, maximum and average values across the 500×500 simulation area points.

Finally, the difference between the Fukuoka and Ibaraki C_{loc} variations for SPV (Figure 12) is much smaller compared to that of the GES C_{loc} differences between the two areas (Figure 8). This is in part due to the large land costs for SPVs, and because GES has to supply stored energy with as little transmission loss as possible. GES is not associated with critical materials like battery technologies, and thus, international trade and macroeconomics are less significant compared to the localized socioeconomics of construction. This shows a third finding, in that GES location-dependent costs are much more sensitive to a specific suburban location than that of SPV. In this study, a bigger metropolitan suburban area with multiple CBDs (Ibaraki) results in lower location-dependent costs for utility-scale GES installations. From a policy perspective, it can be inferred that hybrid SPV-GES systems should be considered in more developed metropolitan suburban areas in curtailment-prone grids than less developed suburban areas, mainly due to a better supply chain infrastructure.

3.3. LCOE Variations of Hybrid SPV-GES Plants

Figure 14 shows the LCOE variations according to Equations (15)–(18) in the two simulation areas. Due to the dominating nature of C_{land} for SPVs, the hybrid SPV-GES LCOE variations in the simulation areas are quite similar in nature to the SPV C_{loc} variations in Figure 12. In Figure 12a, it can be seen that SS1 is affecting the cost-optimized location, as it is directly on a virtual line connecting the Fukuoka CBD to SS1. For Figure 12b, SS2 affects the cost-optimized location, again directly on a virtual line connecting the Ibaraki CBD2 to SS2. Both the optima lie in FPs and not MPs, which reinforces the aforementioned result that flat zones would provide the most optimum installation costs of hybrid systems. Thus, urban planners need not even consider mountainous areas for decentralized suburban installations.

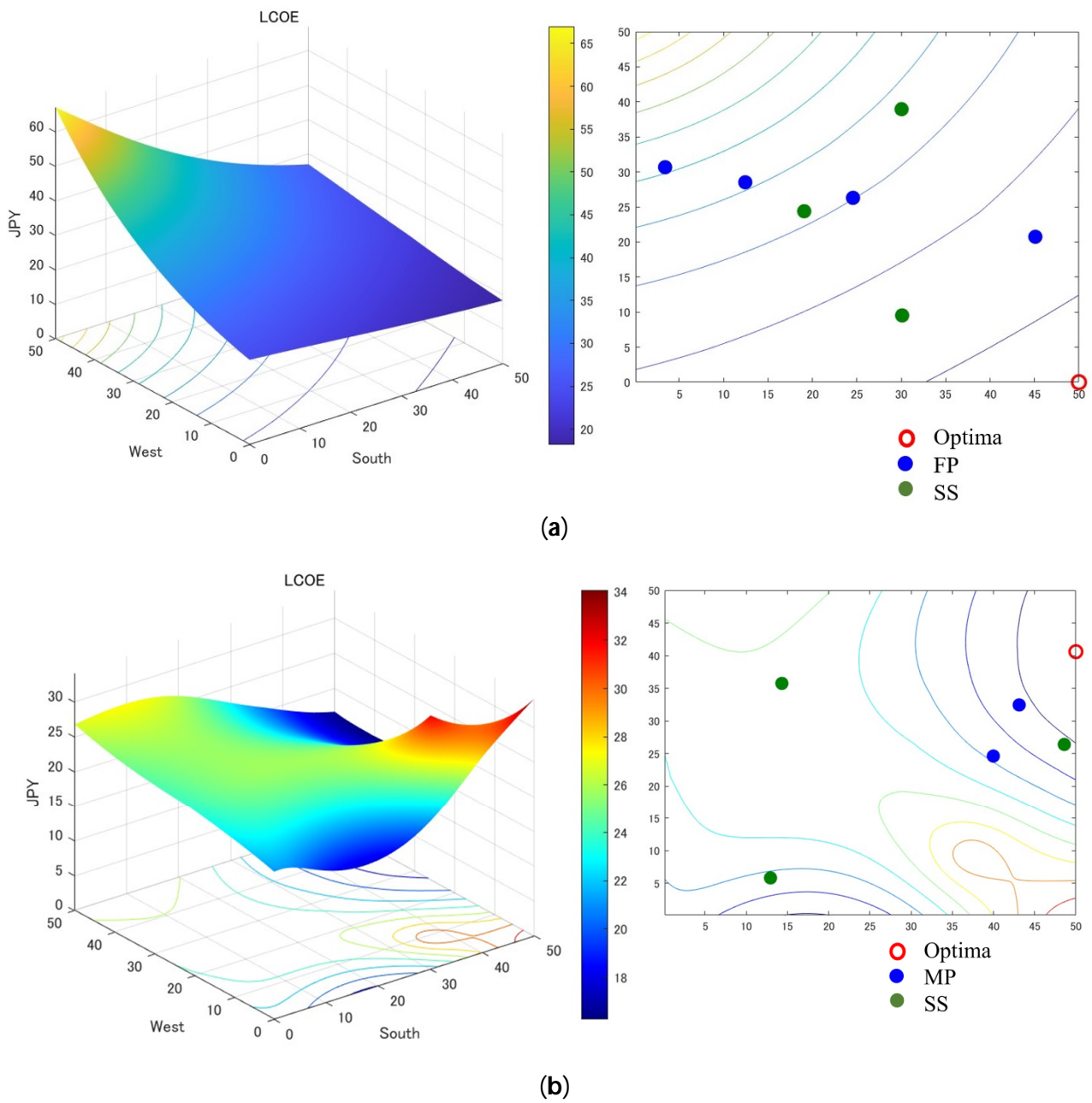


Figure 14. The SPV-GES LCOE variations (in the 500×500 suburban simulation areas for (a) Fukuoka and (b) Ibaraki.

LCOEs can be optimized only at a distance far away from the CBD of a city in the suburban areas of a developed economy. Even in this case, it can be seen that the LCOE levels for Ibaraki (the more developed suburban area) are lower than that of Fukuoka (the less developed mountainous suburban area). This has important implications for geolocating SPV-GES hybrid systems not only within the suburban area at the optimized cost point, but also, they should be located in a more developed metropolitan suburb. This adds knowledge on their economic feasibility in high-curtailment zones to the existing literature on the LCOEs of hybrid systems [7,33].

4. Discussion

4.1. Multi-Criteria Decision for Ranking Cost-Optimal Locations

In the Results Section, it was proposed that a more developed metropolitan suburban area was more suitable for geolocating the hybrid SPV-GES plant, and that flat zones were more economical than mountainous zones. However, to support those interferences, a robustness analysis of the results is required, which is carried out in this section through a multi-criteria decision analysis (MCDA) of the candidate optima locations. Existing MCDA methods like ELECTRE and PROMOTHEE are generally used for large criteria and options for hybrid energy system selections, which range in the hundreds [55,56]. Moreover, such methods are computationally more expensive and cannot be applied to the deterministic MUFSP model introduced in this paper [57].

Therefore, we introduce a new MCDA method for ranking decentralized hybrid systems' location-dependent costs that is based on the order of magnitude of the cost factors (C_{loc}) in the objective functions for SPV and GES (Equation (8)). The introduced method is termed a magnitude-weighted economic (MAWE) MCDA, which is based on an existing additive synthesis method for MCDA ranking [58]. The weights for each criterion are normalized and decided based on the order of magnitude of the cost factors in each candidate location's MUFSP model, given in Equation (19).

$$w_k = \frac{\prod_{i=1}^n m_i}{\sum_{j=1}^n (\prod_{i=1}^n m_{ij})} \quad (19)$$

where w_k is the weight for the k -th criterion, m is the magnitude of the i -th cost factor, j is the option indicator and n is the total number of criteria. Equation (20) reveals the calculation of the rank for the j -th option.

$$R_j = Norm_{0-1} Avg(\sum_{i=1}^n w_k C_i) \quad (20)$$

where C_i is the rating for the i -th cost factor. The rating is given on a scale of 1 to 5 for each cost factor at the respective minima locations. In this case, the global minima of the flat points for the SPV-GES hybrid systems are represented in Fukuoka (FP) and Ibaraki (FP). The local minima of the mountainous regions are extracted from the 500×500 matrices represented by Fukuoka (MP) and Ibaraki (MP). Among the four options, the lowest cost is benchmarked at 5, while the highest cost is given 1. Intermediate ratings are given as per the cost values at the candidate locations. Table 6 reveals the results of the MAWE analysis (Supplementary Materials).

Table 6. Results of MAWE-MDCA for candidate locations of SPV-GES hybrid system.

Criteria	Fukuoka (FP)	Fukuoka (MP)	Ibaraki (FP)	Ibaraki (MP)	Weights
C_{land}	4	2	5	3	0.6433
C_{trans}	4	3	3	2	0.1780
C_{SC}	4	1	5	2	0.1156
C_{exc}	2	5	2	4	0.0632
Normalized Rank	3.8736	2.2521	4.4544	2.7696	

Note: 1 is given to the worst economic performance and 5 is given to the best.

Since distance from CBD is the key economic parameter for each cost factor, it is internalized in the weights of the cost factors. One interesting outcome of the MAWE-MCDA for the hybrid SPV-GES systems is how dominant C_{land} is for SPV, even compared to the significant C_{SC} for GES. The weights of C_{trans} and C_{SC} are quite similar, which explains why the optima for GES is more well-defined than that of SPV. The candidate locations of FPs are more economical than MPs, with Fukuoka (FP) rated at 3.8736, more than one rating point above the Ibaraki (MP) at 2.7696. While confirming the results in the previous section, the following policy order can be confirmed for geolocation suburban SPV-GES hybrid systems:

- a. A flat zone carries much lower location-dependent costs than mountainous terrain.

- b. The flat zone of a more developed suburban area carries a lower land cost and more efficient supply chain, ensuring the most economical optimized location.

4.2. Geometry of the Cost-Optimized Location

The authors of [10] explored a very simple geometrical approximation for determining the cost-optimized location for SPV in the suburban area of a city. The study emphasized a trade-off between two factors, specifically land and transmission costs. As the distance increased from the CBD, land cost decreased exponentially, while transmission cost increased linearly with increasing distance from a substation. The ultimate suggestion of [10] was that the optimized location would lie on a straight line connecting the CBD and the SS, reducing a complex model to a one-dimensional solution. While this was for a developing nation, we found that land cost is much higher in a developed nation (Figure 13), specifically in the costliest metropolitan suburb of Japan, Tokyo [59]. However, we can still find the validity of this approximation for suburban SPV installations in Fukuoka, with land prices being cheaper. To test this, we assumed only SS1 in Fukuoka (Figure 2) and only simulated the dependency of C_{land} and C_{trans} for the simulation area in Fukuoka in Figure 15.

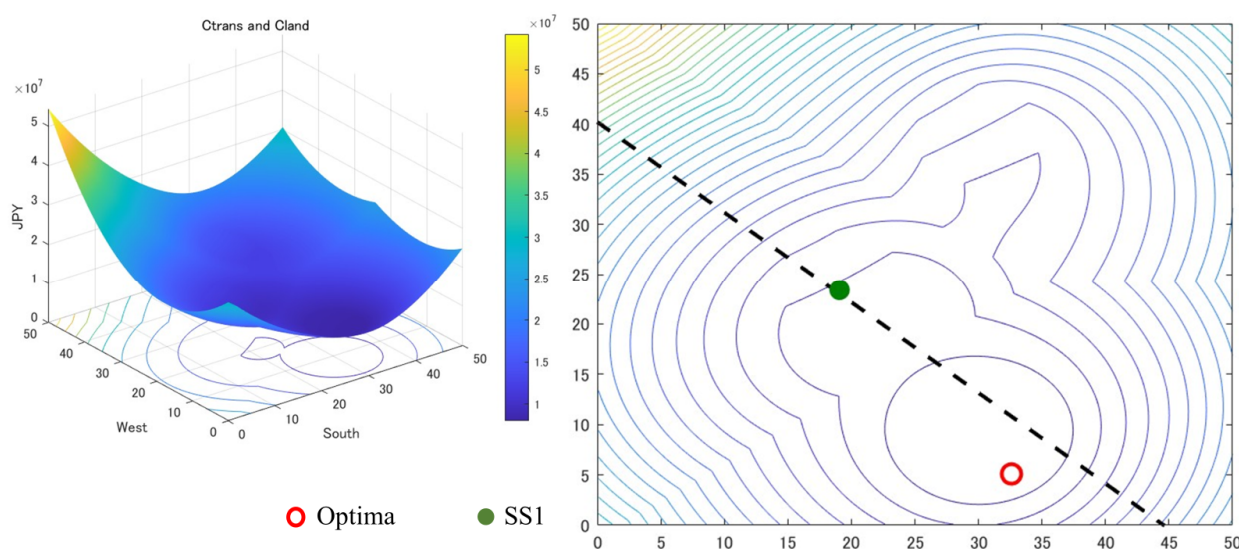


Figure 15. The location-dependent cost variations in the Fukuoka 500×500 simulation area for SPV, based on transmission and land costs and SS1 only (dotted line represents the straight line connecting CBD and SS1 in Fukuoka).

In Figure 15, it can be seen that the optimized cost location in the Fukuoka simulation area is very near the geometrical straight line connecting the CBD and SS1, considering C_{land} and C_{trans} only. Compared to Figure 12a, the optimized location is much nearer to SS1, showing that C_{SC} pushes the optimized location farther away due to mountainous terrain. With this result, the geometrical approximation between land and transmission costs established by [10] in the MUFSP model for suburban SPV installations can be confirmed. This has important implications for VRE integration into suburban areas, specifically in high-land price regions. The previous literature on the economics of decentralized SPV installations has addressed LCOE optimization [33,60–62], while the MUFSP model contributes to geospatial cost optimization affected by urban socioeconomics.

The geometry of the cost-optimized location for GES in Ibaraki, in flat terrain, is the same approximation as Figure 15, with C_{land} replaced by C_{SC} . This is because the supply chain cost function in flat terrain is a linear function (Equation (13)) and is comparable in magnitude to the transmission cost, which is also linear in nature.

The geometry is more complicated in mountainous terrain, however, with C_{SC} being a complex function (Equation (12)). Having concluded that C_{trans} and C_{SC} are the key factors (Figure 9a) in GES C_{loc} , it is observed that the optimal cost location lies on the line connecting CBD and FP2 (say line 1). Thereafter, the perpendicular to a second line connecting the CBD with SS1 (say line 2) intersects with line 1. This point of intersection is where the optimized cost location lies, and the intersection happens at right angles. Figure 16 shows the representative version of this approximation.

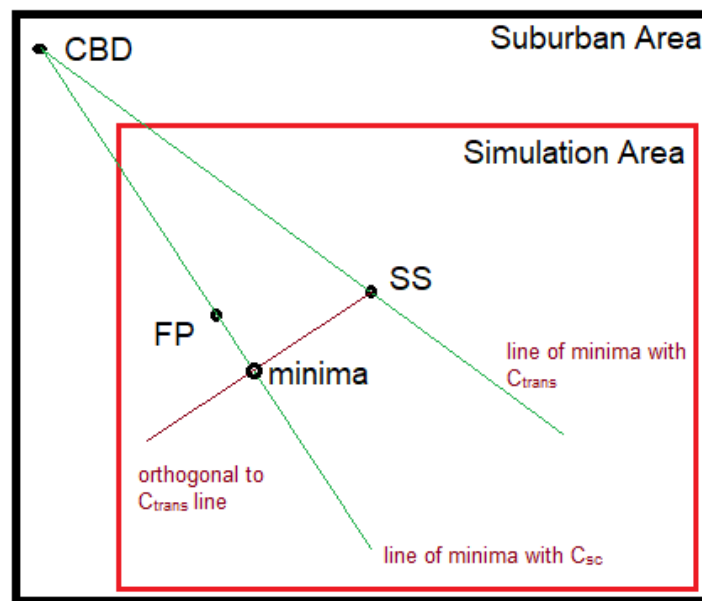


Figure 16. Geometrical approximation of the optimized cost location for a utility-scale GES installation in the suburban mountainous terrain of Fukuoka.

This geometrical approximation has major implications for suburban renewable energy planning and storage deployments in any terrain (since mountainous terrain is revealed to be a non-optimal location). While [10] revealed that SPV geolocation in a suburban region is one-dimensional from a geometric standpoint, this study shows that suburban GES geolocation involves planar (or two-dimensional) geometry. The geometrical approximations in the previous MUFSP model [10] and this advanced MUFSP model have two specific implications on energy policy: (a) the existence of geometrically defined optimized cost points for hybrid systems promises the possibility of curbing curtailment for future decentralized VRE planning even in high-curtailment zones, which was a concern raised by past studies [11–13]; (b) the focal economic centers (CBDs) not only play a vital role in land price hedonic models [10,34,35], but also in co-locating hybrid SPV-GES plants in suburban planning with maximized economic feasibility by minimizing location-dependent costs. The economic focal point, a substation and a portion of flatland in between mountainous terrains are the only factors that need to be considered for suburban GES installation, since C_{SC} in mountainous terrains becomes too high to be economically feasible.

4.3. Is the SPV-GES Hybrid System Economic?

In order to gauge the overall feasibility of GES as a curtailment measure to suburban, decentralized SPV, the LCOS of hybrid GES has to be compared to the LCOS of other storage technologies already existing in Japan. In this case, the capacity and location-dependent costs of GES were based on the assumed curtailment (Table 5) and the hybrid SPV-GES system (Equations (17) and (18)). Figure 17 compares the hybrid GES LCOS with other

energy storage benchmark costs [63] (cost parameters are converted from US dollars to Japanese yen (USD 1= JPY 145 as of 20 March 2024)). Although there is a range of values depending on the installation location within the 2500 km² area, Figure 17 considers the minima to the midpoint values for Ibaraki and Fukuoka. A significant outcome is that GES is cost-competitive with other energy storage technology benchmarks in both the simulated suburban case studies. It can be further seen that the cost-optimized location in Ibaraki carries a lower LCOS than that of Fukuoka. This reconfirms the above conclusion, that developing GES in a more developed metropolitan suburban area can bring the cost down due to the lower price of labor and lower supply chain costs due to better road infrastructure [64], as GES is heavily dependent on supply chain costs. Moreover, the Ibaraki cost-optimized location LCOS is cheaper than all the benchmarks, albeit the benchmarks often inflate the costs without optimizing for socioeconomic factors.

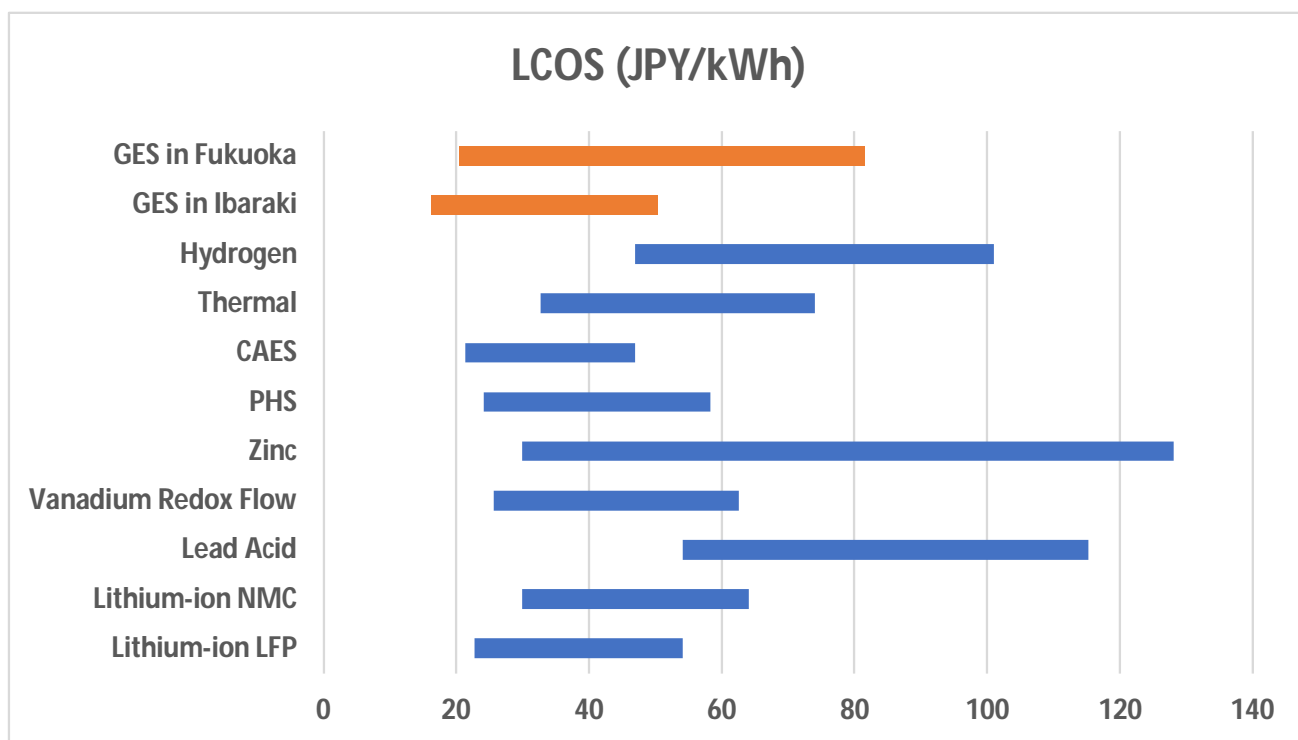


Figure 17. Comparison of the LCOS of GES in the simulated SPV-GES hybrid cases with the LCOS benchmarks of other energy storage technologies in Japan [benchmark data obtained from].

Although this is a simulated scenario, Figure 17 shows the potential for GES to be cost-competitive, specifically over CAES and PHS (which also have competitive LCOS), since the P-GES technology is not limited by geographical conditions like the former two [18,19,21]. Secondly, Li-ion battery technologies (like nickel–manganese–cobalt (NMC) and lithium–ferrous–phosphate (LFP)) have a comparative response time to P-GES, if not faster [65]. However, LFP and NMC depend on critical rare-earth elements, which are very prone to market shocks, and geopolitical conflicts can rapidly drive up the LCOS of such technologies [65]. Thus, the advantages of flexible response times and capacity lie with the cost-competitive P-GES due to the non-existence of critical raw materials. Based on these two reasons, GES can be expected to play a major role in meeting the demand for energy storage for expanding decentralized VREs in curtailment-prone areas.

4.4. Sensitivity Analysis for SPV-GES Hybrid System's LCOE

In this section, we discuss the factors that are most sensitive towards determining the LCOE of the simulated hybrid SPV-GES systems at the cost-optimized points in the two suburban areas. Firstly, the curtailment ratio (k) is considered, which was assumed to be

0.2379 in Table 5. As discussed in Section 2.4, curtailment will increase with decentralized VRE increase, in line with the power generation trajectory of Japan [38]. k is a variable that determines what percentage of the power generated by the SPV is subject to curtailment, and thereby determines P_{GES} (Equation (18)). For example, when $k = 0$, all SPV generation is utilized, and when $k = 1$, the entire SPV generation is curtailed and stored in the GES, which inadvertently increases P_{GES} . Figure 18 shows the relationship between k and the LCOE at the cost-optimized points for the hybrid SPV-GES system. The red marks in Figure 18 represent the LCOE simulation results for $k = 0.2379$ based on Kyushu Electric Power's supply and demand [43]. As ' k ' increases, the LCOE increases exponentially. However, it cannot be concluded that a higher LCOE due to the installation of GES necessarily worsens the profitability of the hybrid plant operation. In fact, higher LCOE may increase the profitability of the plant operation [33,66]. This is because the installation of GES enables the operation of a profit-maximizing energy storage and discharge system, which can generate revenue from the margin of difference in daily electricity prices. In other words, electricity can be stored when electricity prices are low and sold when prices are high. From the above, as long as GES is cost-competitive with other energy storage technologies, it can be a viable curtailment mitigation prospect in suburban areas.

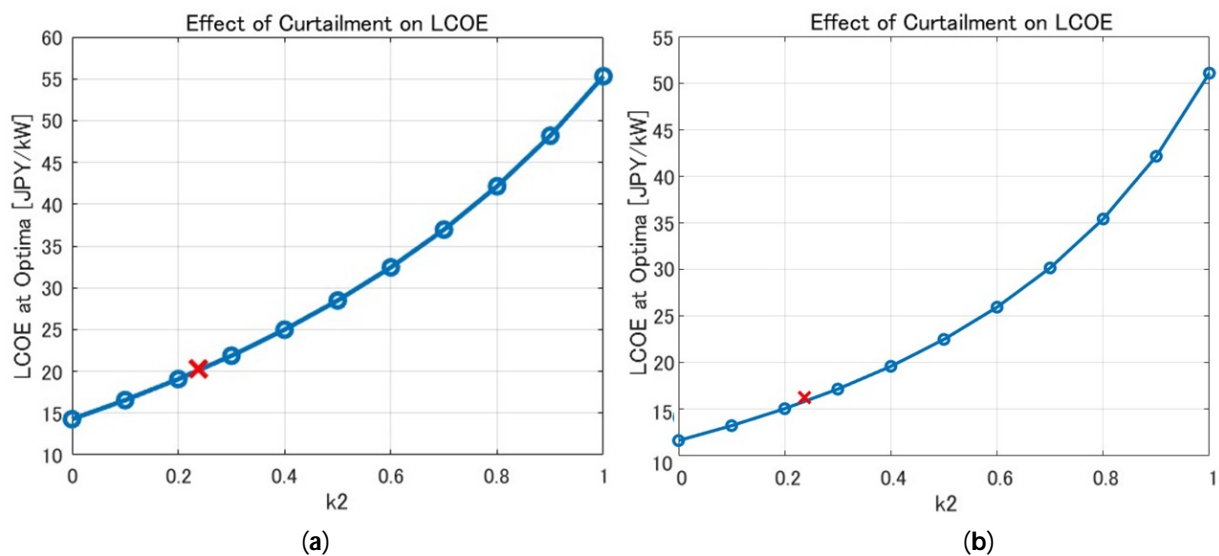


Figure 18. The variation of the LCOE at the cost-optimized locations in the (a) Fukuoka and (b) Ibaraki simulation areas for the SPV-GES hybrid systems with curtailment rate.

In order to verify the absolute profitability of a suburban hybrid SPV-GES system, we consider Figure 19. Here, we consider the difference between the LCOE of a standalone SPV system without GES and the LCOE of the SPV-GES hybrid system at the cost-optimized points. Positive values in the figure indicate that the LCOE has increased due to the introduction of GES, while negative values indicate that the LCOE has decreased due to the installation of GES, meaning that power can be supplied more economically. This is an interesting result; as seen in the mountainous suburban terrain of Fukuoka, the LCOE actually increases with GES introduction for $k < 0.5$, while in the flat suburban Ibaraki terrain, the LCOE difference is close to 0 for $k < 0.5$. In both cases, a hybrid SPV-GES system is very economical for $k > 0.5$. This again proves that mountainous suburban areas with supply chain constraints are not very feasible at low curtailment rates, which adds to the economics of curtailment [15,64]. This study reasonably estimates the point of inflexion for curtailment, where installing GES with VREs in any terrain will be economically feasible ($k > 0.5$).

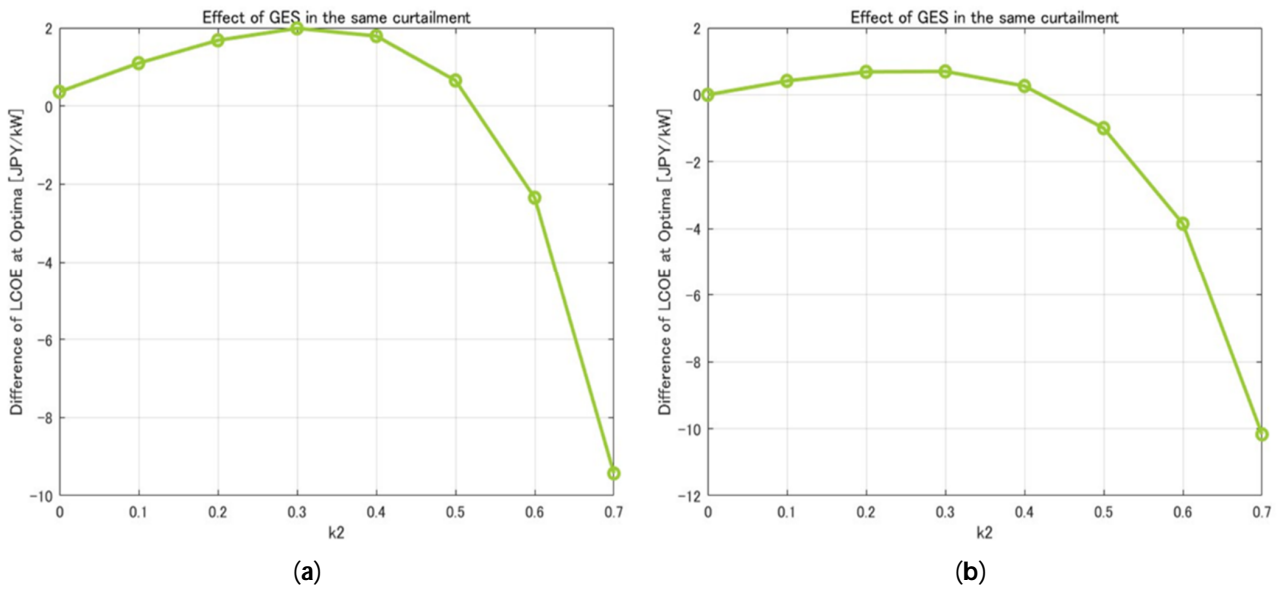


Figure 19. The variation of the LCOE difference between a SPV system and a SPV-GES hybrid system at the cost-optimized locations in (a) Fukuoka and (b) Ibaraki simulation areas with curtailment rate (positive values indicate LCOE has increased due to the introduction of GES; negative values indicate LCOE has decreased due to the introduction of GES).

Figure 20 shows the sensitivity analysis of the effect of discount rate on the LCOE of the SPV-GES systems at the cost-optimized locations. Discount rate is a financially important factor, as the future LCOE of the system depends on discount rate. The higher the discount rate, the larger the range of the LCOE in the future, while the lower the discount rate, the lower median LCOE in the future as well [67]. As seen in Figure 20, as discount rate is increased, there is an almost linear increase in the LCOE of the hybrid SPV-GES system. When the discount rate is 10%, the LCOE more than doubles compared when it is 1%. Thus, the SPV-GES system should ideally be sanctioned when lower discount rates are lower to increase the financial viability of the project.

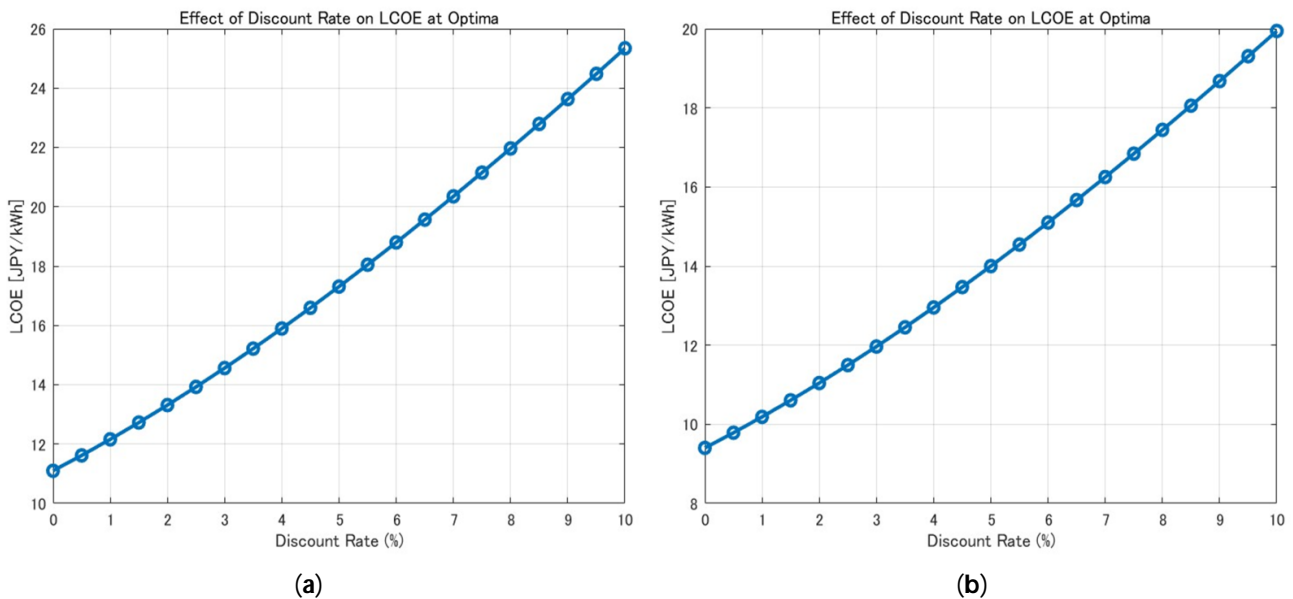


Figure 20. The variation of the LCOE at the cost-optimized locations in (a) Fukuoka and (b) Ibaraki simulation areas for the SPV-GES hybrid systems with discount rate (up to 10%).

4.5. Limitations of This Study

The main limitation is that the MUFSP model developed in this study is only applicable to decentralized suburban VRE-GES projects. This is because the land cost function is comprised of the hedonic approximation model and the supply chain cost function is dependent on urban road infrastructure, which all depend on the socioeconomics of cities. In order for future studies to make this model applicable to rural and remote areas, several approximations of the socioeconomics of such areas need to be researched for determining the location-dependent costs.

Secondly, this study explored the dependency of the LCOE on other factors in a developed economy. The nature of the findings may be vastly different for a curtailment-prone developing region. Future studies may look at either SPV-GES or other VRE-GES hybrid systems and observe the spatial variation in the LCOE in a developing suburban economy using the MUFSP model suggested in this study.

Finally, the capacity of the GES was dependent on the ratio of curtailment, rather than the intermittency of SPV plants. In regions where curtailment is not the main issue, demand analysis needs to be carried out. Future studies can observe the daily and seasonal demand fluctuations and advance the MUFSP model to determine the ideal location for a demand-optimized SPV-GES system that increases both economic feasibility and the capacity factors for decentralized SPV plants.

5. Conclusions

This study analyzes the spatial variations in the location-dependent costs of a hybrid SPV-GES system in two suburban regions of the developed country of Japan using a spatial parameterization model. Location-dependent costs were found to be affected by the socioeconomics of the city, specifically land, transmission, supply chain and excavation (for Piston-GES) costs. The analysis confirmed two hypothesized outcomes in this study: (a) that GES location-dependent costs significantly vary in a suburban area of 2500 km² and (b) that the GES location-dependent costs can be optimized at a specific location due to the trade-offs among the cost functions. Furthermore, this study also analyzed the factors affecting the variations in LCOE and LCOS of decentralized, suburban SPV-GES systems in high-curtailment zones.

The main finding of this study is that the cost-optimized locations for suburban SPV and GES can be geometrically approximated using urban socioeconomics, while SPV can be geospatially optimized on the line connecting the city's CBD and a substation in the suburban area, the GES is optimized on the line connecting the CBD and a flat zone, the flat zone being orthogonal to a line connecting a substation to the CBD. For SPV installations, land and transmission costs were the key trade-off factors, while for GES installations, supply chain and transmission costs were key. Thereafter, it was found that suburban GES systems are more sensitive towards an optimized location than suburban SPV installations.

This study further showed that GES is cost-competitive with other energy storage technologies, specifically in flat terrains due to being geographically dynamic. The absolute LCOE of the SPV-GES system seemed to decrease with increased curtailment, proving that GES is an effective tool for decreasing the LCOE of future decentralized SPV installations. Specifically, it was found that GES introduction reduces the LCOE of an SPV system with curtailment rates above 50% irrespective of the suburban terrain. It was also shown that a lower discount rate reduces the LCOE of a hybrid SPV-GES system tremendously, thereby indicating financial policy measures for lowering the discount rate for future decentralized installations. The main policy recommendations of this study are as follows:

1. Urban socioeconomics renders GES location-dependent costs more sensitive than SPV's. Therefore, the weight of geolocating a hybrid system should be rendered to mechanical storage primarily and VRE secondarily.
2. A mountainous area carries excessive supply chain costs and thus, suburban decentralized SPV-GES hybrid systems should be located in flat zones, despite cheaper excavation costs.

3. Substations are key localizing factors for the suburban cost-optimized location of SPV-GES systems, and therefore, a substation closest to the CBD of the city should be chosen for the grid connection of the system.
4. A more developed suburban area in the vicinity of a metropolis carries a lower LCOE for SPV-GES hybrid systems, and thus in curtailment grids the most developed suburban area should be the candidate location for decentralized energy planning.
5. GES is a viable storage mechanism when curtailment is above a threshold of 40%, or else the LCOE of the hybrid SPV-GES system is uneconomical compared to a standalone SPV system experiencing curtailment.

This study contributes significantly to geolocating economically feasible sites for decentralized hybrid VRE systems, including GES systems, that will be constructed in the vicinity of cities. The outcomes of this study are not only significant for energy planners for achieving affordable and clean energy in the future (SDG 7), but also for urban designers aiming to build sustainable communities and cities (SDG 11), in line with net zero targets.

Supplementary Materials: The following supporting information can be downloaded at: <https://www.mdpi.com/article/10.3390/en17092162/s1>.

Author Contributions: Conceptualization, S.B. and T.H.; methodology, S.B. and T.H.; software, T.H.; validation, S.B. and H.O.; formal analysis, T.H.; investigation, S.B. and T.H.; resources, T.H.; data curation, T.H.; writing—original draft preparation, S.B.; writing—review and editing, S.B. and H.O.; visualization, T.H.; supervision, H.O.; project administration, H.O.; funding acquisition, S.B. All authors have read and agreed to the published version of the manuscript.

Funding: This work was supported by JST SPRING, Grant Number JPMJSP2110, given to Soumya Basu.

Data Availability Statement: The raw data supporting the conclusions of this article will be made available by the authors on request.

Conflicts of Interest: The authors declare no conflicts of interest. The funders had no role in the design of the study; in the collection, analyses, or interpretation of data; in the writing of the manuscript; or in the decision to publish the results.

References

1. Dada, M.; Popoola, P. Recent advances in solar photovoltaic materials and systems for energy storage applications: A review. *Beni-Suef Univ. J. Basic Appl. Sci.* **2023**, *12*, 66. [[CrossRef](#)]
2. Shalwar, P.K.; Gupta, B.; Bhalavi, J.; Bisen, A. Performance Characteristics and Efficiency Enhancement Techniques of Solar PV System: A review. *F1000Research* **2022**, *11*, 1264. [[CrossRef](#)]
3. Kennedy, R. Solar LCOE Now 29% Lower than Any Fossil Fuel Option, Says EY. PV Magazine. 2023. Available online: <https://www.pv-magazine.com/2023/12/08/solar-lcoe-now-29-lower-than-any-fuel-fossil-option-says-ey/> (accessed on 20 March 2024).
4. Yan, J.; Yang, Y.; Elia Campana, P.; He, J. City-level analysis of subsidy-free solar photovoltaic electricity price, profits and grid parity in China. *Nat. Energy* **2019**, *4*, 709–717. [[CrossRef](#)]
5. Bogdanov, D.; Oyewo, A.S.; Mensah, T.N.O.; Nishida, Y.; Saito, T.; Aikawa, T.; Kimura, S.; Gagnebin, M.; Pescia, D.; Shimoyama, T.; et al. Energy transition for Japan: Pathways towards a 100% renewable energy system in 2050. *IET Renew. Power Gener.* **2023**, *17*, 3298–3324. [[CrossRef](#)]
6. Shen, W.; Chen, X.; Qiu, J.; Hayward, J.A.; Sayeef, S.; Osman, P.; Meng, K.; Dong, Z.Y. A comprehensive review of variable renewable energy levelized cost of electricity. *Renew. Sustain. Energy Rev.* **2020**, *133*, 110301. [[CrossRef](#)]
7. Mahaver, V.K.; Rao, K.V.S. Estimation of Levelized Cost of Electricity (LCOE) of 1 MW SPV Plants Installed at 33 Different Locations in Rajasthan, India. In *Advances in Renewable Energy and Electric Vehicles: Select Proceedings of AREEV 2020*; Springer: Singapore, 2022; pp. 199–208.
8. Darling, S.B.; You, F.; Veselka, T.; Velosa, A. Assumptions and the levelized cost of energy for photovoltaics. *Energy Environ. Sci.* **2011**, *4*, 3133. [[CrossRef](#)]
9. Zhang, F.; Deng, H.; Margolis, R.; Su, J. Analysis of distributed-generation photovoltaic deployment, installation time and cost, market barriers, and policies in China. *Energy Policy* **2015**, *81*, 43–55. [[CrossRef](#)]
10. Basu, S.; Ogawa, T.; Okumura, H.; Ishihara, K.N. Assessing the geospatial nature of location-dependent costs in installation of solar photovoltaic plants. *Energy Rep.* **2021**, *7*, 4882–4894. [[CrossRef](#)]

11. Bird, L.; Lew, D.; Milligan, M.; Carlini, E.M.; Estanqueiro, A.; Flynn, D.; Gomez-Lazaro, E.; Holttinen, H.; Menemenlis, N.; Orths, A.; et al. Wind and solar energy curtailment: A review of international experience. *Renew. Sustain. Energy Rev.* **2016**, *65*, 577–586. [[CrossRef](#)]
12. Dumlao, S.M.G.; Ishihara, K.N. Reproducing solar curtailment with Fourier analysis using Japan dataset. *Energy Rep.* **2020**, *6*, 199–205. [[CrossRef](#)]
13. Frysztacki, M.; Brown, T. Modeling Curtailment in Germany: How Spatial Resolution Impacts Line Congestion. In Proceedings of the 2020 17th International Conference on the European Energy Market (EEM), Stockholm, Sweden, 16–18 September 2020; pp. 1–7.
14. Dumlao, S.M.G.; Ishihara, K.N. Weather-Driven Scenario Analysis for Decommissioning Coal Power Plants in High PV Penetration Grids. *Energies* **2021**, *14*, 2389. [[CrossRef](#)]
15. Dumlao, S.M.G.; Ishihara, K.N. Impact assessment of electric vehicles as curtailment mitigating mobile storage in high PV penetration grid. *Energy Rep.* **2022**, *8*, 736–744. [[CrossRef](#)]
16. Shao, X.; Fang, T. Performance analysis of government subsidies for photovoltaic industry: Based on spatial econometric model. *Energy Strategy Rev.* **2021**, *34*, 100631. [[CrossRef](#)]
17. Schmidt, O.; Melchior, S.; Hawkes, A.; Staffell, I. Projecting the Future Levelized Cost of Electricity Storage Technologies. *Joule* **2019**, *3*, 81–100. [[CrossRef](#)]
18. Blakers, A.; Stocks, M.; Lu, B.; Cheng, C. A review of pumped hydro energy storage. *Prog. Energy* **2021**, *3*, 022003. [[CrossRef](#)]
19. Bouman, E.A.; Øberg, M.M.; Hertwich, E.G. Environmental impacts of balancing offshore wind power with compressed air energy storage (CAES). *Energy* **2016**, *95*, 91–98. [[CrossRef](#)]
20. Berrada, A. Financial and economic modeling of large-scale gravity energy storage system. *Renew. Energy* **2022**, *192*, 405–419. [[CrossRef](#)]
21. Berrada, A.; Loudiyi, K.; Zorkani, I. System design and economic performance of gravity energy storage. *J. Clean. Prod.* **2017**, *156*, 317–326. [[CrossRef](#)]
22. Berrada, A.; Loudiyi, K.; Zorkani, I. Sizing and economic analysis of gravity storage. *J. Renew. Sustain. Energy* **2016**, *8*, 024101. [[CrossRef](#)]
23. Emrani, A.; Berrada, A.; Bakhouya, M. Modeling and Performance Evaluation of the Dynamic Behavior of Gravity Energy Storage with a Wire Rope Hoisting System. *J. Energy Storage* **2021**, *33*, 102154. [[CrossRef](#)]
24. Berrada, A.; Loudiyi, K. Modeling and material selection for gravity storage using FEA method. In Proceedings of the 2016 International Renewable and Sustainable Energy Conference (IRSEC), Marrakech, Morocco, 14–17 November 2016; pp. 1159–1164.
25. Fyke, A. The Fall and Rise of Gravity Storage Technologies. *Joule* **2019**, *3*, 625–630. [[CrossRef](#)]
26. Hunt, J.; Zakeri, B.; Jurasz, J.; Tong, W.; Dabek, P.; Brandão, R.; Patro, E.; Đurin, B.; Filho, W.; Wada, Y.; et al. Underground Gravity Energy Storage: A Solution for Long-Term Energy Storage. *Energies* **2023**, *16*, 825. [[CrossRef](#)]
27. Hunt, J.D.; Zakeri, B.; Falchetta, G.; Nascimento, A.; Wada, Y.; Riahi, K. Mountain Gravity Energy Storage: A new solution for closing the gap between existing short- and long-term storage technologies. *Energy* **2020**, *190*, 116419. [[CrossRef](#)]
28. Tong, W.; Lu, Z.; Chen, W.; Han, M.; Zhao, G.; Wang, X.; Deng, Z. Solid gravity energy storage: A review. *J. Energy Storage* **2022**, *53*, 105226. [[CrossRef](#)]
29. Berrada, A.; Emrani, A.; Ameer, A. Life-cycle assessment of gravity energy storage systems for large-scale application. *J. Energy Storage* **2021**, *40*, 102825. [[CrossRef](#)]
30. Alkay, E.; Watkins, C.; Keskin, B. Explaining spatial variation in housing construction activity in Turkey. *Int. J. Strateg. Prop. Manag.* **2018**, *22*, 119–130. [[CrossRef](#)]
31. Chang, C.-T. Multi-choice goal programming model for the optimal location of renewable energy facilities. *Renew. Sustain. Energy Rev.* **2015**, *41*, 379–389. [[CrossRef](#)]
32. Mayfield, E.; Jenkins, J. Influence of high road labor policies and practices on renewable energy costs, decarbonization pathways, and labor outcomes. *Environ. Res. Lett.* **2021**, *16*, 124012. [[CrossRef](#)]
33. Weinand, J.M.; Hoffmann, M.; Göpfert, J.; Terlouw, T.; Schönau, J.; Kuckertz, P.; McKenna, R.; Kotzur, L.; Linßen, J.; Stolten, D. Global LCOEs of decentralized off-grid renewable energy systems. *Renew. Sustain. Energy Rev.* **2023**, *183*, 113478. [[CrossRef](#)]
34. Bera, M.M.; Mondal, B.; Dolui, G.; Chakraborti, S. Estimation of Spatial Association between Housing Price and Local Environmental Amenities in Kolkata, India Using Hedonic Local Regression. *Pap. Appl. Geogr.* **2018**, *4*, 274–291. [[CrossRef](#)]
35. McDonald, J.F.; McMillen, D.P. Employment Subcenters and Land Values in a Polycentric Urban Area: The Case of Chicago. *Environ. Plan. A Econ. Sp.* **1990**, *22*, 1561–1574. [[CrossRef](#)]
36. Morris, J.; Calhoun, K.; Goodman, J.; Seif, D. Reducing solar PV soft costs: A focus on installation labor. In Proceedings of the 2014 IEEE 40th Photovoltaic Specialist Conference (PVSC), Denver, CO, USA, 8–13 June 2014; pp. 3356–3361.
37. World Bank. *PPPs for Policy Making: A Visual Guide to Using Data from the ICP—Chapter 4: Labor Costs, Wages, and Social Safety Nets. Purchasing Power Parities for Policy Making: A Visual Guide to Using Data from the International Comparison Program*; World Bank: Washington, DC, USA, 2021; Available online: https://www.worldbank.org/en/programs/icp/brief/VC_Ch4_1 (accessed on 20 March 2024).

38. Kiko Network. Japan's Path to Net Zero by 2050. 2021. Available online: https://www.kiconet.org/wp/wp-content/uploads/2021/05/NetZero-Report-2050_EN.pdf (accessed on 20 March 2024).
39. Renewable Energy Institute. Proposal for 2030 Energy Mix in Japan (First Edition) Establish a Society Based on Renewable Energy. 2020. Available online: https://www.renewable-ei.org/pdfdownload/activities/REI_Summary_2030Proposal_EN.pdf (accessed on 20 March 2024).
40. Japan Exchange Group, Inc. Topix Index. Available online: <https://www.jpx.co.jp/english/markets/paid-info-equities/historical/01.html> (accessed on 20 March 2024).
41. Ozcan, O.; Ersoz, F. Project and cost-based evaluation of solar energy performance in three different geographical regions of Turkey: Investment analysis application. *Eng. Sci. Technol. Int. J.* **2019**, *22*, 1098–1106. [CrossRef]
42. Kurniawan, A.; Shintaku, E. Estimation of the Monthly Global, Direct, and Diffuse Solar Radiation in Japan Using Artificial Neural Network. *Int. J. Mach. Learn. Comput.* **2020**, *10*, 253–258. [CrossRef]
43. Kyushu Electric Power. Publication of Lineage Information. 2023. Available online: https://www.kyuden.co.jp/td_service_wheeling_rule-document_disclosure (accessed on 20 March 2024).
44. Agency for Natural Resources and Energy. About Solar Power Generation. 2022. Available online: https://www.meti.go.jp/shingikai/santeii/pdf/082_01_00.pdf (accessed on 20 March 2024).
45. Kohsaka, R.; Kohyama, S. Contested renewable energy sites due to landscape and socio-ecological barriers: Comparison of wind and solar power installation cases in Japan. *Energy Environ.* **2023**, *34*, 2619–2641. [CrossRef]
46. PrimRoot. Top 7 Japanese Solar Panel Manufacturers: 2024 Guide. 2024. Available online: <https://primroot.com/japanese-solar-panel-manufacturers/> (accessed on 20 March 2024).
47. Berrada, A.; Loudiyi, K.; Zorkani, I. Dynamic modeling and design considerations for gravity energy storage. *J. Clean. Prod.* **2017**, *159*, 336–345. [CrossRef]
48. Ministry of Land, Infrastructure, Transport and Tourism. 3.4 Re-estimation of the Introduction Potential of Onshore Wind Power Generation. 2020. Available online: <https://www.env.go.jp/content/900449197.pdf> (accessed on 20 March 2024).
49. Ministry of Land, Infrastructure, Transport and Tourism. National Land Numerical Information Download Site. Available online: https://nlftp.mlit.go.jp/ksj/gml/datalist/KsjTmplt-L01-v3_0.html (accessed on 20 March 2024).
50. IRENA. Solar Power Spatial Planning Techniques. 2014. Available online: https://www.irena.org/-/media/Files/IRENA/Agency/Events/2014/Jul/15/9_Solar_power_spatial_planning_techniques_Arusha_Tanzania.pdf?la=en&hash=F98313D5ADB4702FC910B94586C73AD60FA45FDE (accessed on 20 March 2024).
51. Dujardin, J.; Schillinger, M.; Kahl, A.; Savelsberg, J.; Schlecht, I.; Lordan-Perret, R. Optimized market value of alpine solar photovoltaic installations. *Renew. Energy* **2022**, *186*, 878–888. [CrossRef]
52. Hamfelt, A.; Karlsson, M.; Thierfelder, T.; Valkovsky, V. Beyond K-means: Clusters Identification for GIS. In *Information Fusion and Geographic Information Systems: Towards the Digital Ocean*; Springer: Berlin/Heidelberg, Germany, 2011; pp. 93–105.
53. Oğuz, E.; Şentürk, A.E. Selection of the Most Sustainable Renewable Energy System for Bozcaada Island: Wind vs. Photovoltaic. *Sustainability* **2019**, *11*, 4098. [CrossRef]
54. Hahn, H.; Hau, D.; Dick, C.; Puchta, M. Techno-economic assessment of a subsea energy storage technology for power balancing services. *Energy* **2017**, *133*, 121–127. [CrossRef]
55. Arslan, A.E.; Arslan, O.; Genc, M.S. Hybrid modeling for the multi-criteria decision making of energy systems: An application for geothermal district heating system. *Energy* **2024**, *286*, 129590. [CrossRef]
56. Hosseini Dehshiri, S.S. A new application of multi criteria decision making in energy technology in traditional buildings: A case study of Isfahan. *Energy* **2022**, *240*, 122814. [CrossRef]
57. Perzina, R.; Ramík, J. Microsoft Excel as a Tool for Solving Multicriteria Decision Problems. *Procedia Comput. Sci.* **2014**, *35*, 1455–1463. [CrossRef]
58. Qin, Y.; Qi, Q.; Shi, P.; Lou, S.; Scott, P.J.; Jiang, X. Multi-Attribute Decision-Making Methods in Additive Manufacturing: The State of the Art. *Processes* **2023**, *11*, 497. [CrossRef]
59. Tsutsumi, M.; Shimada, A.; Murakami, D. Land price maps of Tokyo Metropolitan Area. *Procedia—Soc. Behav. Sci.* **2011**, *21*, 193–202. [CrossRef]
60. Joshi, S.; Mittal, S.; Holloway, P.; Shukla, P.R.; Ó Gallachóir, B.; Glynn, J. High resolution global spatiotemporal assessment of rooftop solar photovoltaics potential for renewable electricity generation. *Nat. Commun.* **2021**, *12*, 5738. [CrossRef]
61. Huang, D.; Yang, X.; Wang, X. Location and Cost Optimization of Datacenters and Solar Power Plants. In Proceedings of the 2020 4th International Conference on Computer Science and Artificial Intelligence, Zhuhai, China, 11–13 December 2020; ACM: New York, NY, USA, 2020; pp. 240–246.
62. Thapar, S. Centralized vs decentralized solar: A comparison study (India). *Renew. Energy* **2022**, *194*, 687–704. [CrossRef]
63. Pacific Northwest National Laboratory. Energy Storage Cost and Performance Database. 2021. Available online: <https://www.pnnl.gov/ESGC-cost-performance> (accessed on 20 March 2024).
64. Fokkema, J.E. *Supply Chain Decisions for an Adaptive, Decentralized Renewable Energy System*; University of Groningen: Groningen, The Netherlands, 2021.
65. Lebrouhi, B.E.; Baghi, S.; Lamrani, B.; Schall, E.; Kousksou, T. Critical materials for electrical energy storage: Li-ion batteries. *J. Energy Storage* **2022**, *55*, 105471. [CrossRef]

66. Kuckshinrichs, W.; Ball, C.S.; Aniello, G. Levelized profits for residential PV-battery systems and the role of regulatory and fiscal aspects in Germany. *Energy. Sustain. Soc.* **2023**, *13*, 10. [[CrossRef](#)]
67. International Energy Agency. Projected Costs of Generating Electricity 2020. 2020. Available online: <https://www.iea.org/reports/projected-costs-of-generating-electricity-2020> (accessed on 20 March 2024).

Disclaimer/Publisher's Note: The statements, opinions and data contained in all publications are solely those of the individual author(s) and contributor(s) and not of MDPI and/or the editor(s). MDPI and/or the editor(s) disclaim responsibility for any injury to people or property resulting from any ideas, methods, instructions or products referred to in the content.